Chapter 2

Literature Review

Owing to high demanding application of ceramic materials, improvement in properties of these materials to meet the existing / upcoming challenges is in continuous thrust. For example, the lower fracture toughness restricts their wide industrial and medical applications such as, load bearing implants etc. The compunction of ceramics for the crack propagation can be affected by the reinforcement of secondary phases in the ceramic matrix [1]. There are few basic toughening such as, transformation toughening, crack deflection, crack bridging, micro crack toughening etc. occur in ceramics by the addition of secondary phases [2,3]. Apart from these toughening mechanisms, a novel approach to toughen a ceramic by incorporation of piezoelectric secondary phases has been suggested [4]. In this chapter, effect of incorporation of several types of piezoelectric secondary phases on mechanical, dielectric and electrical, antibacterial and in vitro cytocompatibility of bioceramics has been reviewed.

2.1 Introduction

Depending upon the requirements, metals, ceramics, polymers and their composites are being used as prosthetic implants for orthopaedic applications. Generally, the use of metals and their alloys is primary choice for load bearing parts of the human body because of their good mechanical properties e.g., fracture toughness, Young's modulus etc.[5,6]. However, the long lasting applications of the metallic implants are limited due to the corrosion, wear, fibrous tissue encapsulation and mismatch in the modulus of elasticity between bone and implants [5]. Due to chemical inertness of ceramic biomaterials, the use of ceramics is advantageous over metallic implants which can be utilized for longer duration without the requirement of revision surgery. However, the poor fracture toughness of the ceramics raise the serious issue as far as the load bearing

applications are concerned. To improve the fracture toughness of ceramics, number of secondary phases has been incorporated to the ceramic matrix [7 - 14].

Among various bioceramics, Hydroxyapatite (HA) possesses, chemical as well as crystallographic properties, similar to that of the inorganic component of the natural bone [15]. Therefore, HA is extensively used for orthopedic applications [16]. HA has hexagonal crystal structure where hydroxyl ions (OH^-) ion occupies the center of triangle, formed by Ca^{2+} along the c- axis of hexagonal unit cell [Fig. 2.1] [17, 18].

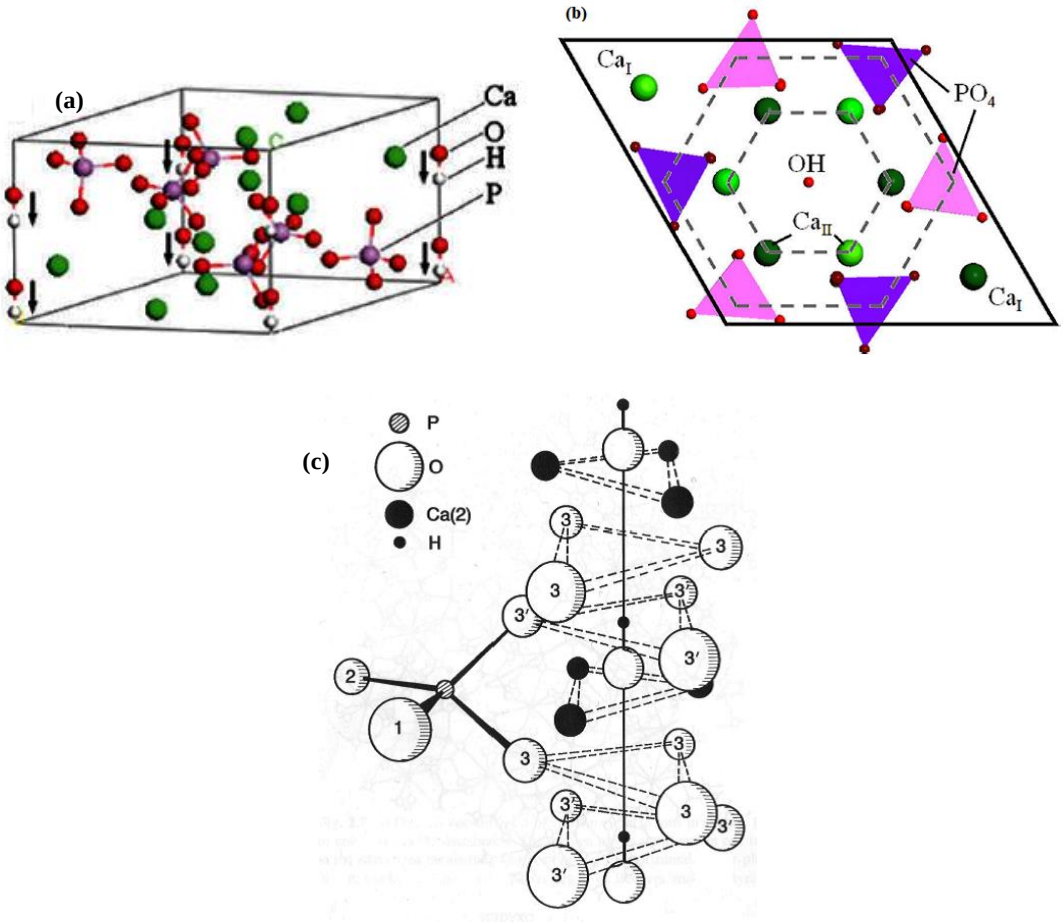

Fig. 2.1 Crystal structure of hydroxyapatite [19,20]

The OH^- ions affect the conduction mechanism in HA [21]. Owing to the interaction between Ca^{2+} and PO_4^{3-} ions and natural bone, HA is being regarded as an excellent biocompatible as well as bioactive material [22 – 25]. Lower mechanical and electrical

properties of HA limit its applications for the orthopedic implantation. Another example of bioceramics is bioactive glasses. 45S5 bioglass (BG; 45 wt. % SiO_2, 24.5 wt. % Na_2O, 24.5 wt. % CaO and 6 wt. % P_2O_5) and 1393 bioglass (53 wt. % SiO_2, 6 wt. % Na_2O, 12 wt. % K_2O, 5 wt. % MgO, 20 wt. % CaO, 4 wt. % P_2O_5) have been widely used for clinical applications due to their excellent biocompatibility and osteoconductivity [26 – 30]. BG forms bond with the bone due to formation of hydroxyapatite layer on its surface with the similar chemical composition as that of the bone and provides augmented osteogenesis by synchronizing the induction and proliferation of cell [31 – 37]. In spite of excellent biocompatibility of these implants, poor electro-mechanical response as well as bacterial infection during surgery or thereafter are among the major concerns which lead to failure of the implants [38].

This chapter reviews one of the novel techniques to enhance the toughness of ceramics with the incorporation of piezoelectric secondary phase in the ceramic matrix. In addition to the piezoelectricity induced major toughening mechanism such as energy dissipation, stress induced domain switching toughening, other toughening mechanisms such as transformation toughening, crack bridging, crack deflection and micro crack toughening also contributes to the total observed toughening of piezo-composites. As far as the piezoelectricity induced toughening is concerned, the poling direction and electrical field parameters affect the toughness of the ceramics. The combined effect of processing parameters and piezoelectricity on toughness of ceramics has been described in this chapter. In addition, the effect of incorporation of secondary piezoelectric phase in different ceramic systems on other mechanical properties such as, hardness and flexural strength are also reviewed. Further, the influence of incorporation of piezoelectric secondary phase on dielectric and electrical, antibacterial as well as cytocompatibity of the ceramics has been reviewed.

2.2 Toughening mechanisms

In general, ceramics have low fracture toughness which fail in catastrophic manner. In order to improve the toughness of ceramics, secondary phases have been incorporated which provide the controlled crack growth. The crack propagates catastrophically in brittle materials under uniform stress, greater than the critical stress σ_f, which is given as [39],

$$\sigma_f = \frac{K_{IC}}{Yc^{\frac{1}{2}}} \qquad (2.1)$$

Where K_{IC}, Y and c are the critical stress intensity factor, geometrical factor, and crack size, respectively. D. Broek [40] as well as Butler and Fuller [41] introduced the R- curve phenomenon for failure of the ceramic materials. The crack propagation or extension occurs when,

$$G \geq R \qquad (2.2)$$

Where, G and R are crack extension energy (strain energy) and resistance for the crack propagation, respectively. Strain energy is related with the stress intensity factor for the plane stress condition as [39],

$$G = \frac{K_I{}^2}{E} \qquad (2.3)$$

Where, E is the Young's modulus of the material. For an applied stress σ and crack with length c, the stress intensity factor K_I can be given as [39],

$$K_I = Y\sigma c^{\frac{1}{2}} \qquad (2.4)$$

For normal fracture of ceramics, where there is no toughening occurs, K_I is taken as the critical stress intensity factor. The measured critical stress intensity factor is equal to the stress intensity factor at the crack tip, $K_{tip\ at\ fracture}$ is denoted for this condition as K_0 i.e., [39],

$$K_{IC} = K_{tip\ at\ fracture} = K_0 \qquad (2.5)$$

The addition of secondary phase in matrix decreases the stress at the crack tip due to the generation of compressive stresses around it [39],

$$\mathbf{K_{tip} = K_I - \Delta K} \qquad (\mathbf{2.6})$$

Where, ΔK is reduction in stress intensity at the crack tip due to toughening.

Now, at the moment when fracture occurs, the applied stress intensity factor is taken as critical stress intensity factor and K_{tip} can be taken as K_0.

$$\mathbf{K_{IC} = K_0 + \Delta K} \qquad (\mathbf{2.7})$$

As shown in the equation (2.7), critical stress intensity factor (fracture toughness) increases with addition of secondary phase. There are few toughening mechanisms which occur due to addition of secondary phases, as briefed in the subsequent sections.

2.2.1 Crack Deflection

When a propagating crack comes into contact with a secondary phase particle, the secondary phase opposes the crack growth, which consequently, decreases the stress intensity factor at the crack tip [42],

$$\mathbf{K_{tip} = \cos^3\frac{\theta}{2} \times K_{app}} \qquad (\mathbf{2.8})$$

Where, θ and K_{app} are the angle of crack deflection and applied stress intensity factor, respectively. The crack deflection increases the crack length and consequently, the fracture toughness. In polycrystalline materials, the average stress intensity factor at the crack tip decreases, due to the deflection of the crack along the weak grain boundaries.

2.2.2 Crack Bridging

In this mechanism, toughening occurs due to secondary phase induced bridging of crack surfaces behind the crack tip which provides a closure force on crack face. The cracks behind the crack tip act as the tiny spring. Owing to this, the stress intensity at the crack tip decreases and consequently, the fracture toughness of the ceramic composite

increases. The fracture toughness [K^c] of the ceramic composite due to crack bridging can be given as [4],

$$\mathbf{K^c = [E^c J^m + E^c \Delta J^{cb}]^{1/2}} \qquad \mathbf{(2.9)}$$

Where, K^c is the total fracture toughness of the ceramic composite, J^m is the fracture energy of the matrix and ΔJ^{cb} is the change in energy associated with the bridging process.

2.2.3 Micro-crack toughening

In this toughening mechanism, the micro-cracks seed in the vicinity of main crack due to which stress at main crack tip decreases. There are few assumptions, based on which micro crack toughening has been formulated. For example, it has been assumed that a crack of semi-infinite length is subjected to an external load in mode I loading condition, as represented by the applied stress intensity factor, K. In addition, the concentration of micro cracks is assumed to be low to avoid the interaction between the micro cracks [43]. Under these conditions, Gong [43] suggested that the variation in stress intensity factor of the main crack due to presence of the single microcrack can be given as,

$$\mathbf{\Delta K = K\left(\frac{c}{8d}\right)^2 G(\theta,\emptyset) + \sigma_R\sqrt{2\pi c}\left(\frac{c}{2d}\right)^2 F(\theta,\emptyset)} \quad \mathbf{(2.10)}$$

$$\mathbf{F(\theta,\emptyset) = \cos\left(\frac{3\theta}{2}\right) + 6\sin\theta\sin\left(\frac{5\theta}{2} - 2\emptyset\right)} \qquad \mathbf{(2.11)}$$

$$\mathbf{G(\theta,\emptyset) = 11\cos\theta + 8\cos(2\theta) - 3\cos(3\theta) + 4\cos(\theta - 2\emptyset) + 2\cos(\theta + 2\emptyset) + 8\cos(2\theta - 2\emptyset) - 6\cos(3\theta - 2\emptyset) - 8\cos(4\theta - 2\emptyset)} \qquad \mathbf{(2.12)}$$

Where, σ_R represents the normal residual stress near the microcrack region, d denotes the distance between the center of micro-crack and main crack tip. Θ is the angle between the x-axis and line connecting the tip of the main crack and Φ denotes the direction of micro-crack. F (Θ, Φ) and G (Θ, Φ) are the explicit functions of (Θ, Φ) [43].

2.2.4 Transformation Toughening

The transformation toughening mechanism can be understood with the help of classical example of tetragonal to monoclinic phase transformation of zirconia (ZrO_2). The change in phase transformation generates a stress around the crack tip which helps in increasing the fracture toughness. Transformation toughening can be understood by observing [2]

(a) The thermodynamic behavior of the material

(b) Fracture toughness variation by stress induced phase transformation

Buljan et al. [44] reported that such transformation results in the generation of a large amount of strain.

$$\varepsilon^t = \begin{pmatrix} \frac{a_m \cos(\frac{90-\beta}{2}) - a_t}{a_t} & 0 & \tan(\frac{90-\beta}{2}) \\ 0 & \frac{b_m - a_t}{a_t} & 0 \\ \tan(\frac{90-\beta}{2}) & 0 & \frac{c_m \cos(\frac{90-\beta}{2}) - c_t}{c_t} \end{pmatrix}$$

Where, a, b and c are the unit cell dimensions with respect to the tetragonal (t) and monoclinic (m) phases. β is the monoclinic angle.

When the resistance during crack propagation is offered by a secondary phase, the strain energy release rate ΔG can be given as [39],

$$\mathbf{\Delta G = 2\, V_f\, \sigma_c \varepsilon^T\, h} \qquad \mathbf{(2.13)}$$

Where, V_f, σ_c, ε^T and h are the volume fraction of secondary phase, stress up to elastic behavior, permanent strain due to tensile loading and distance on either side of an advancing crack, respectively.

The increase in fracture toughness during t → m transformation due to tensile loading can be obtained as [39],

$$\Delta K^{T} = 0.30\, \varepsilon^{T} E V_f h^{\frac{1}{2}} \qquad (2.14)$$

Where, E is the Young's modulus of the material.

Apart from the above toughening mechanisms, the incorporation of piezoelectric secondary phases in ceramic matrix has been suggested to provide the additional toughening, the consequences of which is detailed in the subsequent sections.

2.3 Piezoelectric contribution to the toughening mechanism

Piezoelectric materials generate charges in response to applied mechanical loading and vice-versa. Fig. 2.2 [(a) and (b)] shows the generation of dipoles on the application of either tensile or compressive stresses in the piezoelectric material. This phenomenon is known as direct piezoelectric effect. On the other hand, strain developed in piezoelectric materials in response to applied electric field is known as inverse piezoelectric effect. Owing to piezoelectric effect, domain switching occurs after the application of mechanical loading or electric stimulus which affects the mechanical properties of the piezoelectric ceramics [45].

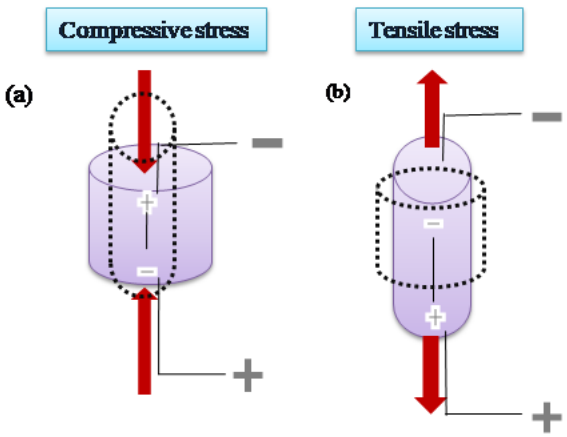

Fig. 2.2 Schematic diagram, representing the direct piezoelectric effect due to (a) compressive and (b) tensile stresses [45].

The dipole generation by mechanical loading and vice- versa in piezoelectric material depend on electromechanical coupling coefficient.

2.3.1 Electromechanical coupling coefficient

The electromechanical coupling coefficient is defined as the ability of the piezoelectric material to transform mechanical energy into electrical energy and vice-versa. The coupling coefficient (K) can be obtained as [46],

$$\mathbf{K^2 = W_{12}^2 / W_1 W_2} \qquad (\mathbf{2.15})$$

Where, W_{12} is piezoelectric energy density; W_1 and W_2 are the mechanical and electrical energy densities, respectively.

2.3.2 Energy dissipation mechanism

All the toughening mechanisms are based on energy balance approach. The general equation to obtain the fracture toughness can be given as [3],

$$\mathbf{K_{IC} = [E^c(J^m + \Delta J)]^{1/2}} \qquad \mathbf{(2.16)}$$

Where, K_{IC} is the total fracture toughness of the ceramic, E_c is the Young's modulus of the composite ceramic, J_m is the energy associated with the crack extension in the ceramic matrix, ΔJ is the change in the energy due to the presence of secondary phase.

During energy dissipation, a part of the mechanical energy is converted into the electrical energy as the crack progresses in the piezoelectric secondary phase. Stress-induced phase transformation or domain wall motion occurs in piezoelectric phase. Owing to which, crack propagation energy decreases that further enhances the fracture toughness of ceramic composite with piezoelectric secondary phase. Therefore, by considering the contribution of piezoelectric secondary phase, the fracture toughness can comprehensively be given as [3],

$$\mathbf{K_{IC}} = [\mathbf{E^c}(\mathbf{J^m} + \Delta\mathbf{J} + \Delta\mathbf{J^{piezo}})]^{\mathbf{1}/\mathbf{2}} \qquad (\mathbf{2.17})$$

Where, ΔJ^{piezo} represents the amount of energy dissipated due to piezoelectric effect.

$$\Delta J^{piezo} = (\text{piezoelectric coeffiecient}) \times (\text{developed electric field}) \times (\text{applied stress})$$

$$\Delta\mathbf{J^{piezo}} = \mathbf{d} \times \boldsymbol{\delta}\mathbf{E} \times \boldsymbol{\delta}\mathbf{X} \qquad (\mathbf{2.18})$$

Where, d, δX and δE are the piezoelectric coefficient, applied stress and developed electric field, respectively.

2.3.3 Domain Switching

Domain switching is defined as the virtue of a ferroelectric material to change the direction of polarization due to the application of electric field or mechanical stresses [47–50]. In ferroelectric materials, domain switching occurs for applied electric field greater than the coercive field as well as for sufficiently large amount of compressive stresses which squeezes the unit cell. It has been reported that only 90˚ domain switching can be achieved with the help of mechanical stresses whereas, the application of electric field provides 90˚ as well as 180˚ domain switching [51]. In zirconia ceramics, tetragonal to monoclinic phase transformation is induced by the stresses acting around the crack tip. The structural transformation results in volumetric changes in the unit cell and consequently, generates the compressive stress. These compressive stresses act on crack tip during it's propagation and shields the tip i.e., arrest the crack propagation. Similarly, for ferroelectrics, like $BaTiO_3$, stress-induced domain switching process (due to the high tensile stresses) near the crack tip, has been suggested as one of the potential toughening mechanisms [52 – 57] The strain mismatch between tetragonal and monoclinic phases occurs due to the rotation of the polar axis of the domains by 90˚. The anisotropic nature of tetragonal phase usually results in compressive stresses. These compressive stresses are generated perpendicular to the crack plane, which is preferred orientation of the c-axis of

the tetragonal $BaTiO_3$ [58]. During crack propagation, the process of domain switching dissipates some amount of energy [59]. The domain switching can also change the mode of stress from tensile to compressive, right before the crack tip [59]. Figs. 2.3 (a) and (b) schematically represent the piezoelectricity induced toughening due to domain switching and energy dissipation.

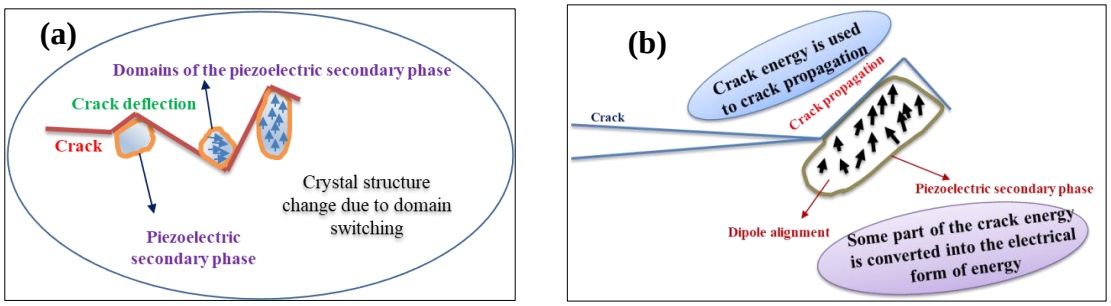

Fig 2.3 Schematic diagram representing the crack deflection

2.3.3.1 Criterion for the domain switching

In presence of both, electrical and mechanical loadings, 90˚ domain switching occurs when the following equation is satisfied [59],

$$\boldsymbol{\sigma_{ij}\Delta\epsilon_{ij} + E_i\Delta P_i \geq 2P_sE_c} \qquad (\mathbf{2.19})$$

Where, σ_{ij} and $\Delta\epsilon_{ij}$ are the stress and strain tensors, respectively. E_i and ΔP_i are electric field and polarization switch vectors, respectively. P_s and E_c are the magnitude of spontaneous polarization and coercive field [59], respectively. The right hand side of the equation shows the threshold energy for polarization switch and is constant for all polarization switches due to electrical and mechanical loadings. It is clearly defined that combination of mechanical and electrical responses must be greater or equal to the product of spontaneous polarization and coercive electrical field. 180˚ domain switching occurs under the following condition [59].

$$\boldsymbol{E_i\Delta P_i \geq 2P_sE_c} \qquad (\mathbf{2.20})$$

The right hand side of the equation shows the threshold energy for polarization switch which is constant for all polarization switches occurring due to electric and mechanical loadings.

2.4 Effect of piezoelectric secondary phase on mechanical properties

In this section, consequences of addition of piezoelectric secondary phase in bioceramics toward improving their mechanical properties have been reviewed.

2.4.1 Influence on fracture toughness of the bioceramics

Chen and Yang [4] suggested a new approach for the toughening of the ceramics by addition of piezoelectric secondary phase. The incorporation of 5 wt. % of $BaTiO_3$ in Al_2O_3 has been reported to enhance the fracture toughness of $BaTiO_3/Al_2O_3$ composite from 3 $MPa.m^{1/2}$ to 5.1 $MPa.m^{1/2}$ [4] In addition processing parameters have also been reported to influence the mechanical properties of ceramics [60 - 64]. The energy dissipation and microcracking toughening are suggested as possible mechanisms for the toughening of the ceramics. In another study, it has been reported that the addition of 5 mol. % of $BaTiO_3$ secondary phase in Al_2O_3 matrix improves the fracture toughness from 4 to 5.1 $MPa.m^{1/2}$ (about 27.5%) at the sintering temperature of 1450˚C due to crack deflection and crack bridging toughening mechanisms [65]. Owing to the reaction between $BaTiO_3$ (above 5 mol. % of $BaTiO_3$) and Al_2O_3, further addition (> 5 mol. %) of piezoelectric $BaTiO_3$ in Al_2O_3 matrix decreases the fracture toughness. Therefore, the piezoelectric secondary phase and base ceramic should be inert to each other. Yang and Chen [3] suggested that the addition of 3 mol. % of $Nd_2Ti_2O_7$ piezoelectric secondary phase in Al_2O_3 matrix (0.03 $Nd_2Ti_2O_7$ / 0.97 Al_2O_3) increases the fracture toughness from about 3.1 to 6.7 $MPa.m^{1/2}$. It has also been reported that the higher concentration of piezoelectric secondary phase (above 3 mol. % of $Nd_2Ti_2O_7$) limits the fracture toughness due to lower relative density. Apart from conventional sintering, spark plasma sintering

(SPS) is the advance technique in which almost theoretical densification can be achieved. Reddy et al. [66] demonstrated that multistage SPS can provide better mechanical properties over conventional sintering. It has been reported that with single stage SPS (SSS), fracture toughness about 4 MPa.$m^{1/2}$ for Al_2O_3 has been achieved. For two stage SPS (TSS), its value increases to about 5.6 MPa.$m^{1/2}$. Almost similar value of fracture toughness has been obtained with multi stage SPS (MSS). Dubey et al. [67] reported that multistage SPSed HA - 40 wt. % $BaTiO_3$ shows the increase in fracture toughness of 132 % with respect to monolithic HA. In another study, SPSed Al_2O_3 - 5 mol. % $BaTiO_3$ shows the fracture toughness of 6.04 MPa.$m^{1/2}$ whereas, this value for pure Al_2O_3 was obtained to be 4 MPa.$m^{1/2}$ [68]. Zhan et al. [69] demonstrated that SPSed Al_2O_3 - 7.5vol% $BaTiO_3$ shows the maximum fracture toughness of 5.36 MPa.$m^{1/2}$ among the composition, including 5, 7.5, 10, 15 vol. % of $BaTiO_3$ content in Al_2O_3 whereas the fracture toughness for pure α-Al_2O_3 was about 3.3 MPa.$m^{1/2}$. It has been suggested that the fracture toughness of the ferroelectric ceramics is also associated with the domain switching of ferroelectric phase [70 - 74]. Liu et al. [75] reported that the incorporation of 5 vol. % of $LiTaO_3$ secondary phase in Al_2O_3 matrix, enhances the fracture toughness of $LiTaO_3/Al_2O_3$ composite up to 4.1 MPa.$m^{1/2}$ which further enhances by addition of 20 vol. % of $LiTaO_3$ from 4.1 to 4.5 MPa.$m^{1/2}$ using hot pressing while, the hot isostatic pressed samples exhibited fracture toughness value of 5.4 MPa.$m^{1/2}$ and the value of fracture toughness decreases by further addition of secondary phase [Fig. 2.4 (a)].

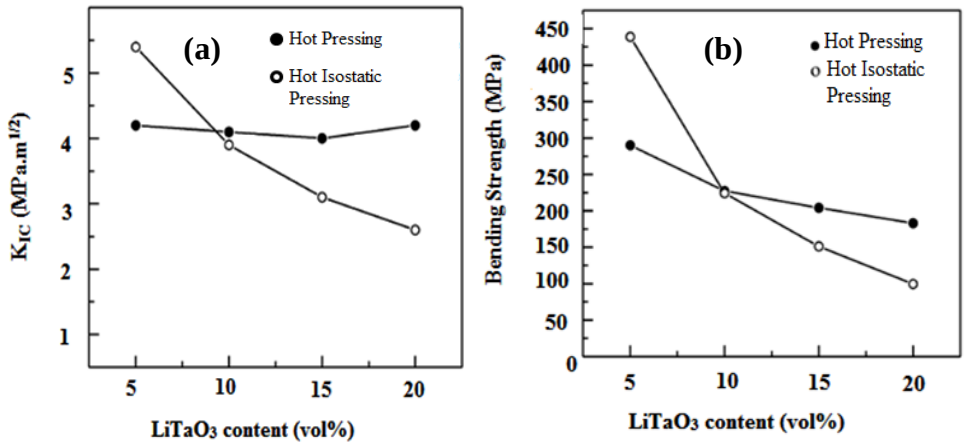

Fig.2.4. Variation of (a) fracture toughness and (b) bending strength of Al_2O_3 with $LiTaO_3$ content in Al_2O_3- $LiTaO_3$ composite [84].

Energy dissipation due to domain switching in piezoelectric secondary phase [76], crack deflection and microcracking has been suggested as the toughening mechanisms [43].

Another bioceramics, Magnesia are being used in valve and pump components, bushings and wear sleeves, industrial tooling applications etc. where the high strength and toughness is required. Rattanachan et al. [77] reported that the addition of 10 vol. % of $BaTiO_3$ as the piezoelectric secondary phase in MgO enhances the fracture toughness of the MgO – 10 vol. % $BaTiO_3$ composite from about 1.5 ± 0.15 to 1.86 ± 0.26 MPa.m$^{1/2}$ without any polarization. After polarization, the MgO – 10 vol. % $BaTiO_3$ composite shows remarkably enhanced value of the fracture toughness of upto about 2.2 MPa.m$^{1/2}$, in the direction parallel to the poling direction. The domain switching has been suggested as one of the toughening mechanisms [78 - 82].

3Y-TZP has been extensively used in dental filling applications because of its reasonable mechanical properties as well as aesthetic aspects. However, they are very delicate to stress concentrations near pre-existing small defects such as, pores or cracks during dental fixation [83]. The addition of piezoelectric $BaTiO_3$ [84, 85] and $Sr_2Nb_2O_7$ [86] secondary phases have been reported to enhance the fracture toughness of 3Y-TZP ceramics. Yang

et al. [84] demonstrated the fracture toughness value of about 5 MPa.m$^{1/2}$ for 3Y-TZP-3 mol. % $BaTiO_3$ composite. By increasing the $BaTiO_3$ content (>5 mol. % of $BaTiO_3$) in 3Y-TZP matrix, fracture toughness of $BaTiO_3$/3Y-TZP composite has been reported to decrease drastically because of transformation of t-ZrO_2 phase to m-ZrO_2 phase [87,88]. Li et al. [89] demonstrated that the addition of 10 mol. % of piezoelectric $BaTiO_3$ secondary phase in 3Y-TZP enhances the fracture toughness value from about 8.5 MPa.m$^{1/2}$ to 10 MPa.m$^{1/2}$ of SPSed 3Y-TZP- 10 mol. % $BaTiO_3$ composite. Chen et al. [86] reported that the addition of 1 mol. % piezoelectric $Sr_2Nb_2O_7$ secondary phase in 3Y-TZP enhances the fracture toughness of the composite from 6 MPa.m$^{1/2}$ to 13 MPa.m$^{1/2}$. Phase transformation toughening mechanism [90] and energy dissipation, associated with piezoelectricity have been suggested as the responsible toughening mechanisms. Liu and Chen [90] reported that the addition of 5 mol. % of $BaTiO_3$ secondary phase in 8% doped Yttria fully stabilized Zirconia (8Y-FSZ) enhances the fracture toughness from about 3.1 MPa.m$^{1/2}$ to 6.1 MPa.m$^{1/2}$ at the sintering temperature of 1475˚C. Crack bridging and crack deflection has been suggested as the toughening mechanisms. Liu et al. [91] reported that the addition of 15 mol. % of $LiTaO_3$ secondary phase in Al_2O_3 matrix significantly enhances the fracture toughness of $LiTaO_3$/Al_2O_3 composite. It has been reported that when crack propagates, high stress concentrates at the crack tip. When this stress concentration exceeds a threshold limit, the domains switching in piezoelectric secondary phase occurs [92- 94]. Figs. 2.5 and 2.6 demonstrate the deflection in crack path due to the addition of piezoelectric $LiTaO_3$ secondary phase in Al_2O_3 matrix. Energy dissipation due to domain switching, crack deflection and micro-crack toughening has been suggested as possible mechanisms for the toughening of the ceramic systems. [95 97]

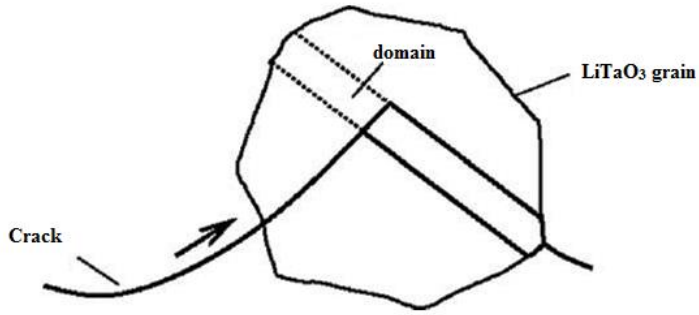

Fig 2.5 Schematic diagram illustrating the crack deflection at domain boundaries in piezoelectric $LiTaO_3$ grain [91]

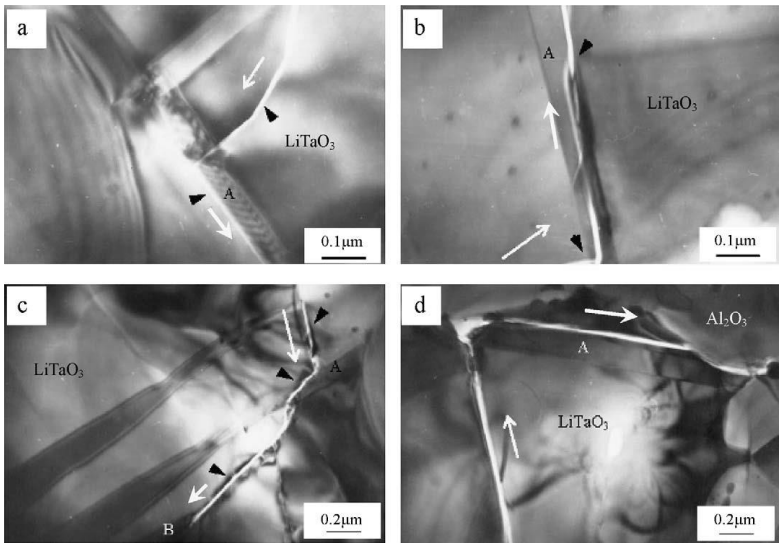

Fig 2.6 TEM micrographs demonstrating the crack deflections and branching in $LiTaO_3$ grains in Al_2O_3-15 $LiTaO_3$ ceramic composite: (a) Crack deflection of about 90˚ (b) crack deflection less than 90˚and crack branching (c) crack deflection less than 90˚ and (d) crack deflection more than 90˚ [91].

Ferroelectric ceramics can change the polarization direction by the application of electric field and can be depolarized by the mechanical stresses [47- 50]. It has been reported that only 90˚ domain switching in piezoelectric material by mechanical loading while electric field switches the domain by180˚ [Fig. 2.7] [51, 98]

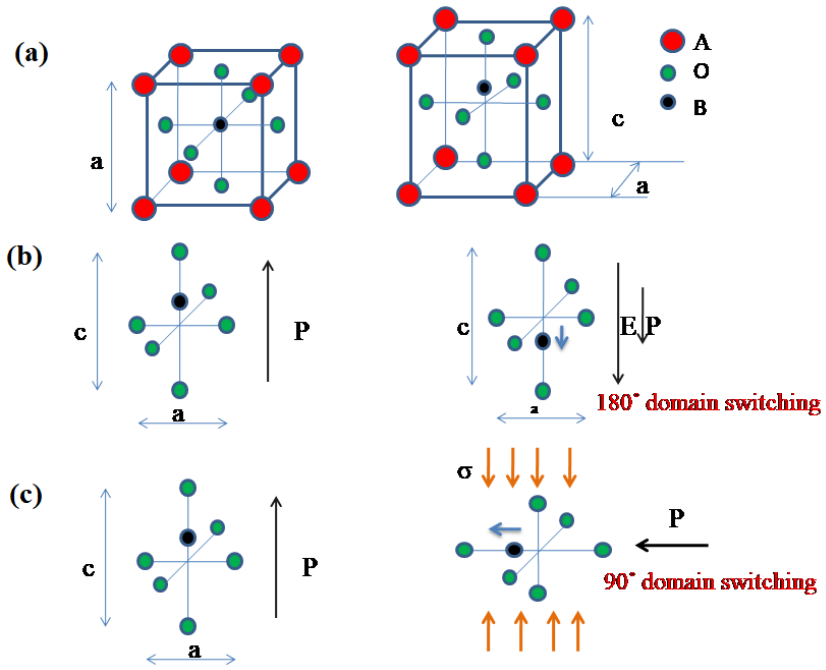

Fig. 2.7 Schematic diagram representing the (a) cubic to tetragonal phase transition, (b) 180˚ polarization switching induced by an externally applied electric field above the coercive field and (c) 90˚ polarization switching induced by a compressive stress [51].

For ferroelectrics, like $BaTiO_3$, stress induced domain switching has been suggested as one of the potential toughening mechanisms due to the tensile stresses near the crack tip region [52] The tetragonal phase generates the compressive stress due to the strain mismatch in the matrix. For the crack propagation, domain switching dissipates some amount of energy [59]. On the other hand, domain switching can change the mode of stress from tensile to compressive right before the crack tip [60].

2.4.2 Effect of piezoelectric secondary phase on other mechanical properties of bioceramics

In addition to the improvement in fracture toughness, the piezoelectric secondary phases have been observed to modify the number of other mechanical properties such as compressive strength, hardness and bending strength. Xiao et al. [99] reported that the addition of $BaTiO_3$ secondary phase in Al_2O_3 matrix enhances the hardness as well as

bending strength. It has been observed that the maximum hardness (Hv = 137) and flexural strength (269 MPa) for 5 mol. % of $BaTiO_3$ secondary phase in Al_2O_3 has been obtained among 0, 0.5, 1, 5, 10, 20 mol. % of $BaTiO_3$ piezoelectric secondary phases in Al_2O_3. Yang et al. [84] reported that the addition of 3 mol. % of $BaTiO_3$ in 3Y-TZP matrix increases the Vickers hardness from about 8 to 12 GPa. Li et al. [85] reported that the addition of 14 mol. % of piezoelectric $BaTiO_3$ secondary phase in 3Y-TZP enhances the elastic modulus from about 230 GPa to 250 GPa. In another study, the addition of 3% and 5% mol. % $BaTiO_3$ in Al_2O_3 exhibited the hardness values 9.28 and 7.26 GPa at 1400°C while at 1450˚C the values were 8.49 and 7.14 GPa obtained, respectively [65]. However, monolithic Al_2O_3 has the hardness of 17.59 GPa at 1500˚C [65]. Undesirable reaction between $BaTiO_3$ and Al_2O_3 has been suggested as one of the possible reasons for such variation in hardness values [77] Beyond the 5 mol. % of $BaTiO_3$ detrimental effect on fracture toughness of Al_2O_3-$BaTiO_3$ composite has been observed [65]. Rattanachan et al. [77] reported that addition of $BaTiO_3$ as the piezoelectric secondary phase in MgO decreases the hardness value of the composite MgO – 10 vol. % $BaTiO_3$ by almost 13 % than monolithic MgO. Liu et al.[90] reported that the addition of 5 vol. % $LiTaO_3$ as the secondary phase in Al_2O_3 enhances the flexural strength up to 438.7 MPa for hot isostatic pressed Al_2O_3 – 5 vol. % $LiTaO_3$ composite samples [Fig. 2.4 (b)]. Further, the addition of secondary phase $LiTaO_3$ in Al_2O_3, detoriated the value of flexural strength. Li J. et al [89] reported that the SPSed 3Y-TZP - 10wt% $BaTiO_3$ exhibits hardness and elastic modulus value of about 16 GPa and 250 GPa, respectively, than that of conventionally sintered samples (about 13 GPa and 190 GPa, respectively). In another study, Dubey et al. reported that multistage SPSed HA - 40wt % $BaTiO_3$ composite exhibits the enhanced hardness value from 5.9 to 6.5 GPa. Similarly, compressive strength enhanced from about 70.2 to 138.3 MPa [76]. Liu and Chen [90] reported that the addition of 5 mol. % of

$BaTiO_3$ in 8Y-FSZ enhances the Young's modulus upto about 176 GPa and hardness value upto 11.6 GPa at 1475°C. On the application of electric field, domain switching occurs due to which the mechanical properties of the piezoelectric ceramics can be tailored [100].

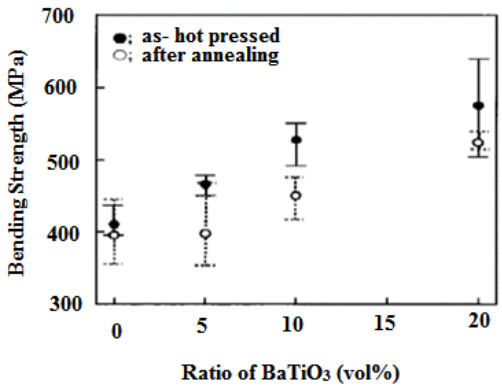

Fig. 2.8 Variation of bending strength of MgO as a function of $BaTiO_3$ content.

Nagai et al. [10] reported that the addition of 20 vol. % of the $BaTiO_3$ piezoelectric secondary phase in MgO ceramic enhances the bending strength of the MgO/$BaTiO_3$ composite from 320 MPa to 520 MPa, for the samples which was annealed at 1250˚C and from 420 MPa to 570 MPa for hot pressed (1350°C with 40 MPa) samples [Fig. 2.8].

2.5 Effect of piezoelectric secondary phase on dielectric and electrical properties of bioceramics

The functional performance of orthopedic implant has been demonstrated to improve by increasing the electrical activity of composite system. The natural bone comprises of collagen and minerals, mainly calcium phosphate components, with the ability of self – healing [101]. For bone remodeling and regeneration, calcium phosphate bioceramics are the potential osteoinductive and osteoconductive substitutes [102]. In addition, it is well known that the natural bone is electrically active tissue [103] which (electrical activity) play an important role in controlling it's metabolic processes [104]. The dielectric behavior of human bone was reported for the first time in 1950s [105-106]. The dielectric

constant [107,108] and ac conductivity [67] of human bone are reported to be 8-10 and 10^{-10} $ohm^{-1}.cm^{-1}$, respectively. Behari et al. [109] observed that bone possesses low dielectric constant value at higher frequency (~GHz) due to breakage of H-bond separation in collagen and apatite. In another study, Wei and Yates [110] suggested that the conductivity of HA has been enhanced up to 10^{-2} S cm^{-1} by the incorporation of yttrium at the same processing temperature (700 °C). Dubey et al. [67] reported that the room temperature dielectric constant and ac conductivity of HA are 12 and 1.5×10^{-9} $(\Omega\ cm)^{-1}$. At low temperature (< 150°C), the dielectric constant variation is due to structural defects like O_2 molecules as well as O^- and OH^- ions. Whereas, at high temperatures (> 300°C), the movement of thermally induced defects are responsible for polarization. Shi et al.[111] demonstrated that the addition of 20 vol. % of Ti_3SiC_2 in HA enhances the dielectric constant of upto 700 (at 1 kHz and room temperature) for Ti_3SiC_2 / HA composites. Dubey et al. [25] reported the dielectric constant and loss for HA-40 wt. % $BaTiO_3$ and HA-60wt. % $BaTiO_3$ to be 21, 38 and 0.01 and 0.02, respectively at room temperature. Bowen et al. [112] reported that the dielectric constant and loss values for HA-40 wt. % $BaTiO_3$ (1 Hz) are varied from almost 900 to 750 within the frequency from 0.1 Hz to 1 MHz. The ac conductivity of HA-40 wt. % and HA-60 wt. % $BaTiO_3$ has been reported to be order of 10^{-10} and 10^{-9} $(ohm\ cm)^{-1}$, respectively [25]. In another study, Dubey et al. [113] reported that the room temperature dielectric constant and loss for HA-40 wt. % $BaTiO_3$ are 18.7 and 0.001, respectively, at 1 kHz. However, HA – 40 wt. % $CaTiO_3$ composite samples exhibited dielectric constant and loss values of almost 22.7 and 0.003, respectively. The values of ac conductivity has been reported to be 1.6×10^{-11} $(ohm\ cm)^{-1}$ and 4×10^{-11} $(ohm\ cm)^{-1}$ for HA-40 wt. % $BaTiO_3$ and HA-40 $CaTiO_3$, respectively.

Pisitpipathsin et al.[114] reported that the incorporation of 15 wt. % barium calcium zirconate titanate ($Ba_{0.92}Ca_{0.08}Zr_{0.05}Ti_{0.95}O_3$, BCZT) in BG increases the dielectric constant of BG - 15 BCZT composite by almost 50 %. While, the composites exhibited the dielectric loss within the range of 0.1 – 0.4 at 1 kHz. In another study, Tigunta et al. [115] demonstrated that the incorporation of 10 wt. % of piezoelectric barium zirconium titanate ($BaZr_{0.05}Ti_{0.95}O_3$, BZT) in calcium phosphate bioglass (40 wt. % CaO – 45 wt. % P_2O_5 – 15 wt. % Na_2O, CPG) enhances the dielectric constant of BG-10 BZT composite by about 13 times. However, the further addition of piezoelectric BZT secondary phase in BG decreases the dielectric constant. Apart from piezoelectric secondary phase, Porwal et al.[116] demonstrated that the addition of 5 vol. % of graphene nano plates in BG increases the electrical conductivity of BG – 5 vol. % GNP composite by almost 9 times of monolithic BG. Eldin and Bockris [117,118] reported that the electrical conductivity of the sodium silicates glass can be influenced by varying the concentration and mobility of alkali ions like sodium ions (Na^+) [Fig. 2.9].

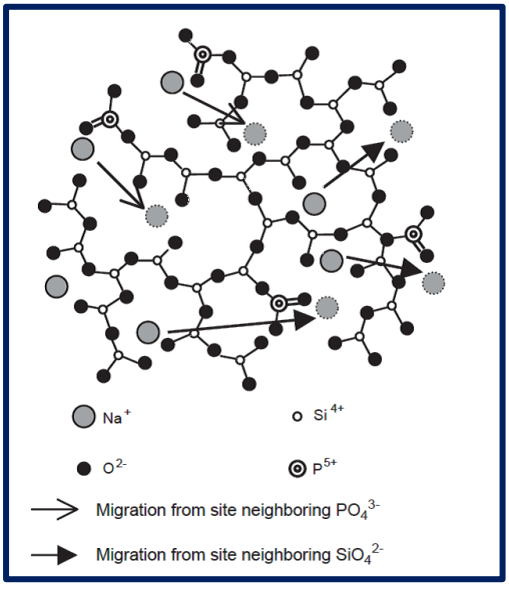

Fig. 2.9 Schematic diagram representing sodium ion migration to interstitial position in sodium silicate glass [119].

It has been reported that the sodium potassium niobate ($Na_{0.5}K_{0.5}NbO_3$; NKN) (ε_r = 657) is also a promising candidate as the piezoelectric secondary phase to enhance the electrical as well as mechanical properties of HA [120- 121]

2.6 Effect of piezoelectric secondary phase on antibacterial behavior of the bioceramics

Swain et al. [122] reported that polarized HA - 60 wt. % $BaTiO_3$ reduces the viability of *S. aureus*, *E. coli* and *P. aeruginosa* bacteria by almost 47%, 46% and 41%, respectively. While, 43%, 35% and 34% of reduction in viability of the *S. aureus*, *E. coli* and *P. aeruginosa* bacterial cells, respectively are observed for polarized HA - 40 wt. % $BaTiO_3$ composite. It has been observed that the polarized samples offer better antibacterial response as compared to unpolarized samples [123]. In another study, Kumar et al.[123] reported that about 88% populations of E. coli bacterial cells have been damaged by polarization treatment sample of $Ba_{0.85}Ca_{0.15}Ti_{0.9}Zr_{0.1}O_3$ (BCTZO) at 2.9 kV/mm for 30 min. It has been proposed that surface charge induced by the poling enhances the antibacterial behavior of the samples [124].

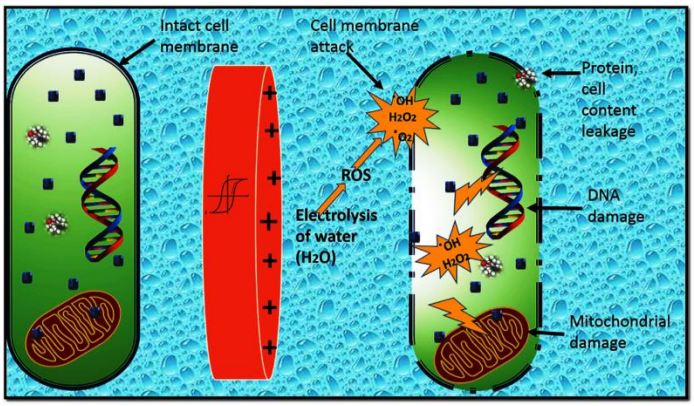

Fig. 2.10 Schematic diagram representing the ROS generation on charged surface and consequently, bactericidal effect [124].

It has been reported that negatively charged surface is expected to repel the bacterial cells and interact with positively charged surfaces of the sample due to electrostatic interaction

[124]. The interaction of positively charged surfaces with bacteria has been reported to depolarize the cell membrane. Such depolarization leads to the abrupt change in the permeability of membrane which results in cell death. Because gram positive and gram negative bacterial cells possess the negative charge. Gram positive bacterial cells have the outer thick layer of peptidoglycan and gram negative bacterial cells have thin but embedded with lippopolysaccharide. These layers possess the negative charge [125]. Therefore, gram negative bacteria possess more negative charge than gram positive bacteria [126]. It has been suggested that the polarized surfaces increase the generation of reactive oxygen species (ROS) which induces antibacterial response. ROS contains peroxides, superoxides, hydroxyl radical singlet oxygen, alpha oxygen etc. which are toxic in nature and damage the bacterial cells [Fig. 2.10] [127,128]. Tan et al. [129] observed the polarization of potassium sodium niobate (KNN) at 25 kV/cm for 30 min enhances the ROS generation by S. aureus bacterial cells which provide more antibacterial response. It has been reported that generation of ROS occurs because of micro electrolysis due to surface charge on the samples [Fig. 2.11].

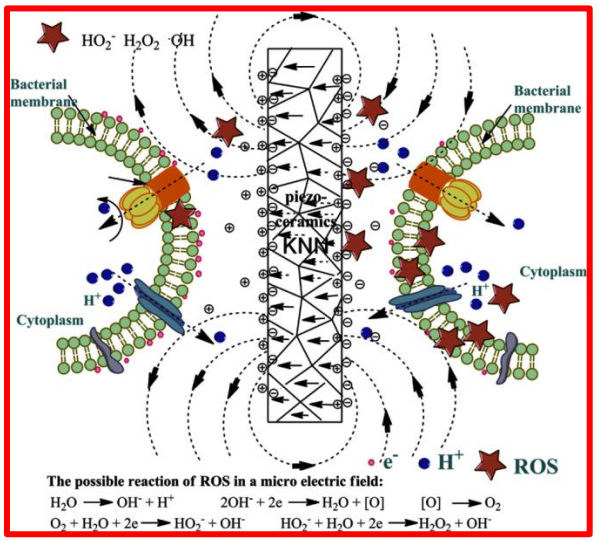

Fig. 2.11 Schematic diagram representing the ROS generation due to surface charge induced by the polarization of potassium sodium niobate (KNN) sample [130].

It has also been reported that piezoelectric KNN with high piezoelectric coefficient (80 pC/N) exhibited almost 100 % antibacterial behavior [130].130

Apart from the piezoelectric secondary phase, a number of studies have been performed to improve the antibacterial response of bioceramics using Ag, Cu, Zn and Mg as the secondary phases [131 - 134]. Afzal et al. [135] reported that the addition of 5 wt. % of Ag in HA composite reduces the bacterial adhesion by almost 64.9 % and 78.8 % for gram positive and gram negative bacteria, respectively.

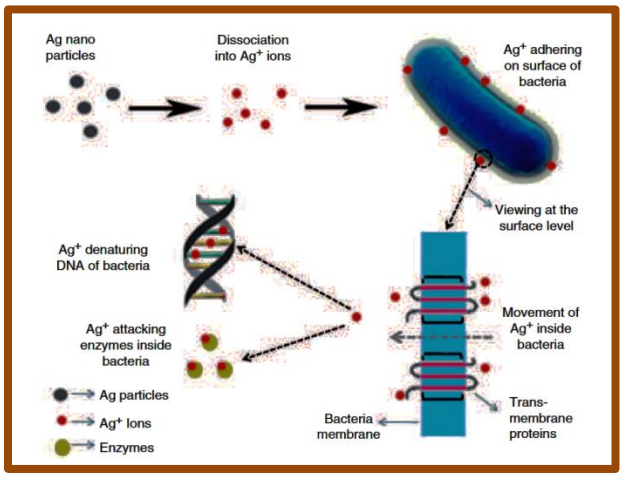

Fig. 2.12 Schematic diagram representing antibacterial action of Ag particle towards bacterial cells [136]

It has been reported that Ag^{+} ions damage the surface of bacterial cells [Fig. 2.12]. These ions are diffused to the cytoplasm of bacterial cells which lead to inhibition of bacterial growth and kill the bacterial cells. In another study, Pandey et al. [136] reported that the incorporation of 2.5 wt. % of Ag in HA reduces the E.coli and S. aureus bacterial cell population up to almost 61 % and 53 %, respectively, for HA-2.5 wt. % Ag composite samples than that of monolithic HA. When Ag ion come in to contact with bacterial enzymes, it provides hurdle for synthesis of proteins which leads to bacterial death.[136] Grenho et al. [137] demonstrated that the addition of 10 wt. % of ZnO in HA reduces the bacterial colony by 35 % whereas incorporation of 30 wt. % of ZnO results in almost 60

% reduction in population of E coli bacterial cells. It has been proposed that such type of antibacterial behavior in HA-ZnO composite is due to generation of reactive oxygen species (ROS). In another study, Boda et al. [138] reported that the addition of 10 wt. % ZnO in HA reduces the S aureus bacterial adhesion by 70 % whereas the pure HA exhibit almost 60 % reduction in the presence of DC electric field of intensity 1 V/cm.

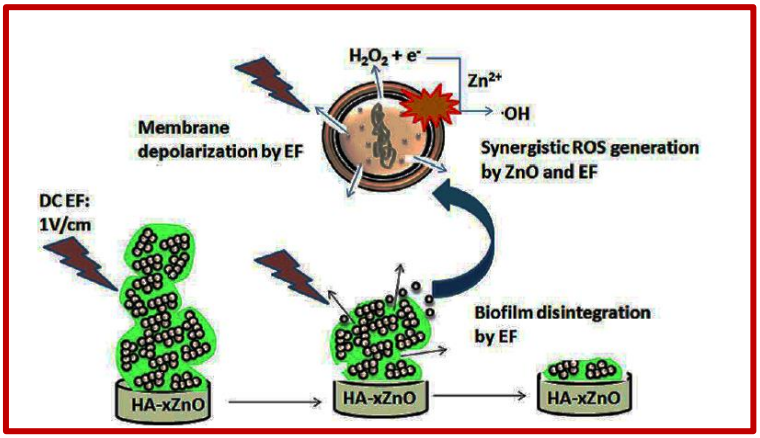

Fig. 2.13 Schematic diagram representing biofilm disintegration on HA-ZnO surface due to externally applied electric field [139].

It has been reported that the application of external electrical field reduces the metabolic response of the bacteria and inhibits the bacterial growth [Fig. 2.13]. This occurs due to the variation in the potential of bacterial membranes.[138] In another study, it has been reported that the application of dc field of 3 kV/cm for 2 h reduces the viability of S. aureus bacterial cells by about 42 and 28 % on positively and negatively charged surface of monolithic HA, respectively [139]. In another study, it has been reported that the addition of 3 wt. % of Ag in 76S bioglass shows better antibacterial response than monolithic 76S bioglass against gram negative bacteria (Escherichia coli) due to the interaction of Ag^+ ions with lippopolysaccharide layer in the membrane of bacterial cells and destructs the cells by affecting their metabolic activities [140, 141]. In another study, Jurczyk et al. [142] suggested that about 90 % population of S. mutants and S. aureus bacterial cells has been reduced by the addition of 1.5 wt. % of Ag on Ti - 45S5 BG due

to the exchange of Ag^+ ions with the body fluid. However, addition of these bacterial agents beyond a certain amount leads the concern of their toxic effects. Microbiologists suggest that the antibiotics can be one of the potential alternatives to keep away from the bacterial infection. However, certain bacteria develop resistance against antibiotics over a period of time [143]. As the bacterial membranes are electrically charged, the development of surface charges on implants can be anticipated as an appealing alternative to induce antibacterial response.

2.7 Effect of piezoelectric secondary phase on cytocompatibity of the bioceramics

Apart from mechanical, dielectric and electrical as well as antibacterial behavior, the cytocompatibilty of the piezoelectric implant material is one of the important concerns. $BaTiO_3$ is reported to be potential candidate for clinical application. It has been demonstrated that HA - $BaTiO_3$ composite shows the excellent mechanical as well as cytocompatility behaviour [144]. Owing to piezoelectricity, HA- $BaTiO_3$ generates surface charge due to stress, which promoted the formation of new bone i.e. supports osteogenesis [145]. Zhang et al. [145] reported that the addition of 70 wt. % of $BaTiO_3$ in HA enhances the cell proliferation by about 201 % for HA-70 $BaTiO_3$ composite, cultured with L929 cell line. In another study, Dubey and Basu [146] demonstrated that addition of 40 wt. % of $BaTiO_3$ in HA enhances the cell proliferation (in terms of mean optical density) for HA - 40 $BaTiO_3$ composite samples cultured with L929 cell line [Fig.2.14].

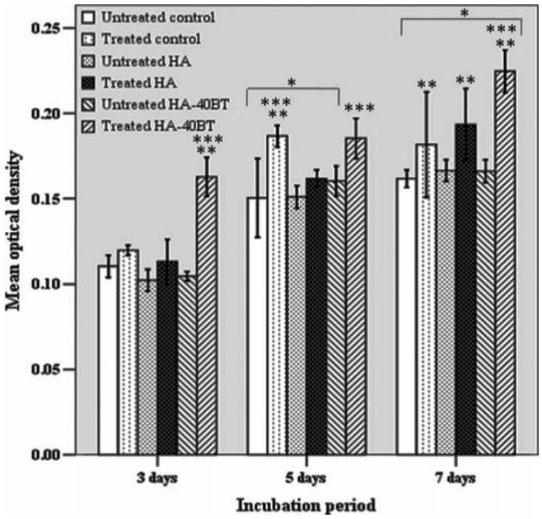

*Fig. 2.14 Cell viability of untreated and electric field treated (E-field strength: 1 V/cm) L929 cells, cultured on control disk, HA and HA–40 wt. % $BaTiO_3$ composite. Asterisk * shows the significant difference among the samples incubated for 5 and 7 days with respect to that incubated for 3 days ** and ***Significant differences among the samples of same incubation period with respect to untreated control disk and HA, respectively at $P < 0.05$ [147].*

Irrespective of sample type and incubation period, cell growth is also affected by electrical polarization. It has been reported that negatively charged samples with electrical polarization enhances the cell proliferation. Fig. 2.15 illustrates the proposed mechanism for cell adhesion on negatively and positively charged HA - 20 wt. % $BaTiO_3$ and HA - 40 wt. % $BaTiO_3$ composite samples. It has been suggested that with increase in the content of $BaTiO_3$ secondary phase, cell growth and proliferation enhances, after polarization treatment [147].

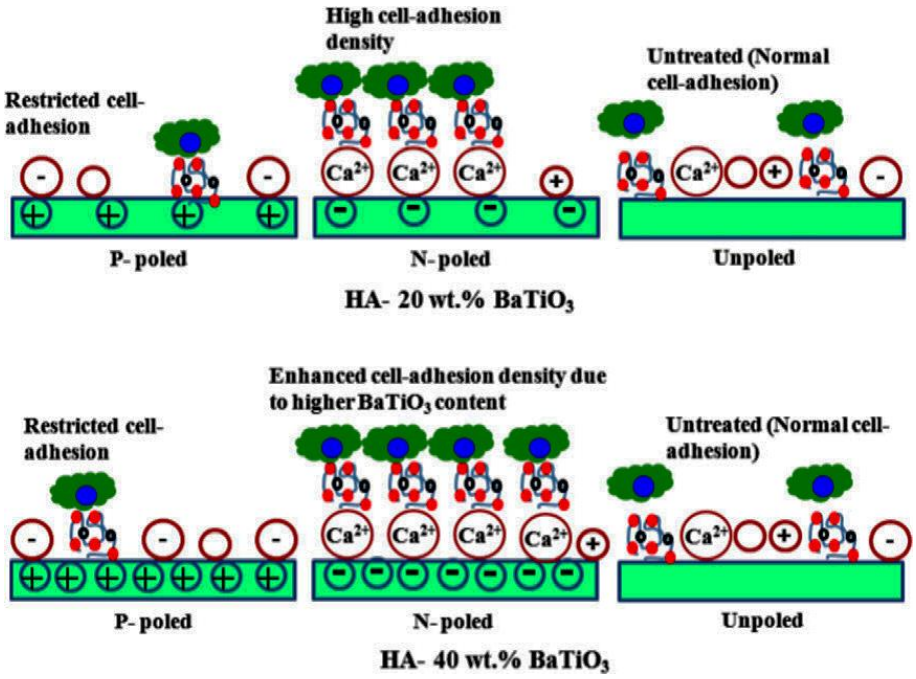

Fig. 2.15 Schematic diagram, illustrating the mechanism of cellular response on positively and negatively charged HA - 20 wt. % $BaTiO_3$ and HA - 40 wt. % $BaTiO_3$ composites [148].

Baxter et al. [148] reported that the cell proliferation has been enhanced on polarized HA-$BaTiO_3$ composite than unpolarized sample, while cultured with Saos-2 human osteoblast cells. A significant enhancement in cell growth was observed after 7 days of incubation. Similar result was observed for positively and negatively charged HA and HA-BT composite samples. Kumar et al. [123] reported that surface charge, generated by poling, promote the cell attachment as well as cell proliferation e.g., negatively and positively charged HA enhances the metabolic activity as compared to the uncharged HA cultured with MC3T3-E1 cells. Kobayashi et al. [149] suggested that the negatively charged surface, induced by the polarization of HA, enhances the osteobonding than unpolarized surface and also demonstrated that the formation of new bone occurs on the negatively charged surface within 7 days of implantation which is directly bonded to HA crystals. It has been suggested that the electrostatic force due to the negatively charged surface charge promote the activation of formation of new bone with specific orientation of bone

layer [151]. In another study, Itoh et al. [150] demonstrated that the polarization of HA increases mineralization process in which negatively charged surface initially absorbed the Ca^{2+} ions then anions like HPO_4^{2-}, HCO_3^- and OH^- ions were attracted by Ca^{2+} which promote mineralization.

Calcium phosphate cement (CPC) and magnesium phosphate cement (MPC) have also been reported to be possible candidate for orthopaedic applications [151 - 156] Wu et al. [157] synthesized the magnesium calcium phosphate cement (MCPC) and reported that cytocompatibility of MCPC was higher than the monolithic CPC and MPC when cultured with MG 63 cell line. After 7 days of incubation, optical density of cells for MCPC has been increased by 150 % than that of 2 days of incubation. In another study, it has been observed that the addition of piezoelectric 20 wt. % and 40 wt. % $BaTiO_3$ in CPC decreases the cell proliferation, cultured with OB-6 pre-osteoblast cell [158]. Duan et al. [159] reported that addition of 1.5 wt. % of graphene oxide (GO) in nano-rod HA (NRHA) enhances the cell proliferation as compared to control samples, when cultured with MC3T3-E1 cells. The mineralization of HA crystals occurs in three steps. First the calcium ions were absorbed and nucleated on HA nanocrystals. Second, transition from nanocrystals into plate shaped nanocrystals and at the last formation of cluster of HA nanocrystals occurs [Fig. 2.16].

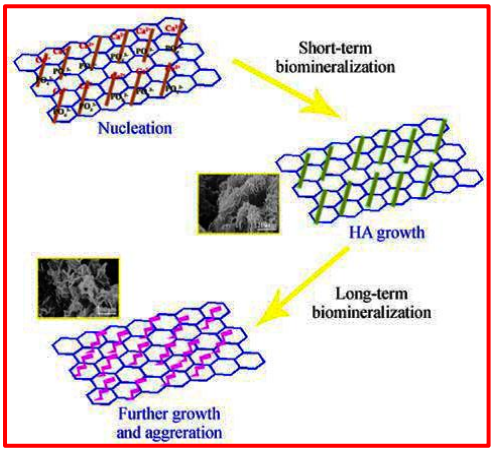

Fig. 2.16 Schematic diagram representing the mineralization of HA in SBF [161].

In another study, Zhu et al. [160] demonstrated the cytocompatibilty of HA-GN and HA-MWCNT composite samples, cultured with MC3T3-E1 cells. It has been observed that the addition of 2 wt. % graphite nano (GN) sheets in HA hindered the cell proliferation while incorporation of 2 wt. % multi walled carbon nano tubes (MWCNT) stimulated the cell proliferation. It has been suggested that fiber structured substrates absorbed more protein than sheet structured substrates.

2.7 Summary

As a closure, this chapter reviews the effects of incorporation of piezoelectric secondary phase in various ceramic matrices, on their mechanical properties such as, fracture toughness, compressive strength, hardness and bending strength. Towards this perspective, the potentiality of piezoelectric secondary phases in providing the additional toughening by means of converting the mechanical energy into electrical energy have been elaborately discussed. Further, the influence of surface charge in inducing the antibacterial response has also been reviewed. In contrast, the cellular response can be improved by inducing the surface charges by polarization as well as by the application of external electrical stimulation during cell growth and proliferation.

As the electrical activities of bone play an important role in controlling various metabolic processes of natural bone, the development of materials for orthopedic applications requires careful consideration of such electro-active response in addition to the reasonable mechanical properties. Therefore, in addition to biocompatibility, bone mimicking mechanical, dielectric and electrical properties of developed implants can be suggested to a better alternative, as far as the long term success of prosthetic implant is concerned.

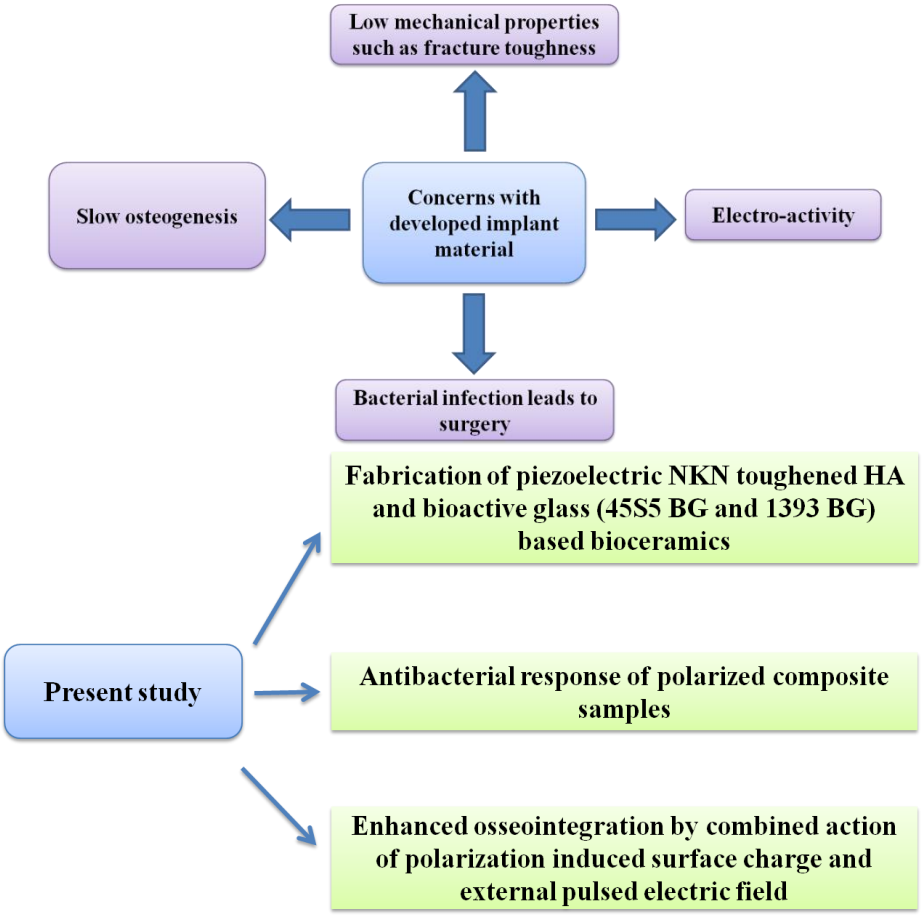

Fig. 2.17 Diagram, representing the novelty of present work

References

1. A. G. Evans, "Perspective on the Development of High-Toughness Ceramics", *Journal of the American Ceramic Society*, **73** (21) (1990) 187-205.

2. F. F. Lange, "Transformation toughening, Part 1 Size effects associated with the thermodynamics of constrained transformations," *Journal of Materials Science,* **17** (1982) 225-234.

3. B. Yang, X.M. Chen," Alumina ceramics toughened by a piezoelectric secondary phase," *Journal of European Ceramic Society,* **20** (2000) 1687-1690.

4. X. M. Chen, B. Yang, "A new approach for toughening of ceramics," *Materials Letters*, **33** (1997) 237-240.

5. C. M. Agrawal, "Reconstructing the Human Body Using Biomaterials," *Journal of Minerals, Metals & Materials Society***, 50** (1) (1998) 31–35.

6. R. Richard, W. Siegel. Gretchen E. Fougere. Mechanical properties of nanophase metals, *NanoStructure Materials* **6** (1995) 205 - 216.

7. T. Kosmac, M. Drofenik, B.Malic, S. Besenicar, M. Kosec, V. Krasevec, S. Somiga "The Influence of Dispershed ZrO_2 Particles on The Properties of Some Electronic Ceramic", *Advanced Ceramics II*, (1988) 29–44.

8. T. Sekino, T. Nakajima, S. Ueda, and K. Niihara, "Reduction and Sintering of a Nickel–Dispersed-Alumina Composite and Its Properties," *Journal of the American Ceramic Society,* **80** (5) (1997) 1139–48.

9. X. M. Chen, L.S. Yang, "Toughening of PZT Piezoelectric Ceramics by In-Situ Complex Structures," *Journal of the European Ceramic Society,* **18** (1998) 1059-1062.

10. T. Nagai, H. J. Hwang, M. Yasuoka, and M. Sando, "Preparation of a Barium Titanate–Dispersed-Magnesia Nanocomposite,"*Journal of the American Ceramic Society,* **81** (2) (1998) 425–28.

11. T. Yamamoto, H. Igarashi & K. Okazaki, "Electrical and mechanical properties of SiC whisker reinforced PZT ceramics," *Journal Ferroelectrics,* **63** (1985) 281-288.

12. L. M. Navarro, P. Recio, J. R. Jurado, P. Duran, "Preparation And Properties Evaluation Of Zirconia-Based/Al_2O_3 Composites As Electrolytes For Solid Oxide Fuel Cell Systems," *Journal Of Materials Science,* **30** (1995) 1949-1960.

13. M. J. Reece, F. Guiu, "Estimation of toughening produced by ferroelectric/ferroelastic domain switching", *Journal of the European Ceramic Society,* **21** (2001) 1433-1436

14. M. H. Fathia, A. Hanifia, V. Mortazavi, "Preparation And Bioactivity Evaluation Of Bone-Like Hydroxyapatite Nanopowder," *Journal of Materials Processing Technology,* **202** (2008) 536–542.

15. M. Jarcho, "Calcium Phosphate Ceramics as Hard Tissue Prosthetics. *Clinical Orthopaedics and Related Research,* **157** (1981) 259–278.

16. L. L. Hench, "Bioceramics," *Journal of the American Ceramic Society,* 81(1998) 1705–1728.

17. K. Yamashita, K. Kitagaki, T. Umegaki, "Thermal-Instability and Proton Conductivity of Ceramic Hydroxyapatite At High-Temperatures," *Journal of the American Ceramic Society,* **78** (1995) 1191–7.

18. M. P. Mahabole, R.C. Aiyer, C.V. Ramakrishna, B. Sreedhar, R.S. Khairnar, "Synthesis Characterization And Gas Sensing Property Of Hydroxyapatite Ceramic," *Bulletin of Materials Science,* **28** (2005) 535–45.

19. S. Alexander and A. D. Alexander, “Hydroxyapatite Vibrational Spectra and Monoclinic to Hexagonal Phase Transition,” *Journal of Applied Physics,* **117** (2015) 074701.

20. J. C. Elliott, “Structure and Chemistry of The Apatites and Other Calcium Orthophosphates.” *ISBN 97814832903,* **17** (1994).

21 K. Yamashita, H. Owada, T. Umegaki, T. Kanazawa, T. Futagamu, “Ionic-Conduction In Apatite Solid-Solutions,” *Solid State Ionics,* **28** (1988) 660–3.

22. I. Sopyan, M. Mel, S. Ramesh, K.A. Khalid, “Porous Hydroxyapatite for Artificial Bone Applications,” *Science and Technology of Advanced Materials,* **8** (2007) 116–123S.

23. K.Y. Lee, M. Park, H.M. Kim, Y.J. Lim, H.J. Chun, H. Kim, S.H. Moon “Ceramic Bioactivity: Progresses, Challenges and Perspectives,” *Biomedical Materials,* **1** (2006) 31–7.

24. K.A.Hing, S.M. Best, K.E. Tanner, W. Bonfield, P.A. Revell, “Mediation of Bone Ingrowth in Porous Hydroxyapatite Bone Graft Substitutes,” *Journal of Biomedical Materials Research Part A,* **68** (2003) 187–200.

25. A. K. Dubey, B. Basu, K. Balani,R. Guo,A. S. Bhalla, “Dielectric and Pyroelectric Properties of HAp-BaTiO3*Composites,*” *Ferroelectrics,* **423** (2011) 63–76.

26. L.L. Hench, "The challenge of orthopaedic materials", *Current Orthopaedic*, **14** (2000) 7-15.

27. M.V. Regí,C. Ragel, A.J. Salinas, "Glasses with Medical Applications, *European Journal of Inorganic Chemistry*, **6** (2003) 1029-1042.

28. J. Wilson, S.B. Low, "Bioactive Ceramics for Periodontal Treatment: Comparative Studies in the Patus Monkey," *Journal of Applied Biomaterials*, **3** (1992) 123-129.

29. S. M. Carvalho, C. Moreira, A. C. X. Oliveira, A. A. R. D Oliveira, E. M. FLemos, M. M. Pereira, "Bioactive Glass Nanoparticles for Periodontal Regeneration and Applications in Dentistry", *Nanobiomaterials In Clinical Dentistry*, (2019), 351-383.

30. H. Tripathi, S.P. Singh, K.A. Sampath, M. Prerna, J. Ashish. "Studies on Preparation and Characterization of 45S5 Bioactive Glass Doped with (TiO2 + ZrO2) as Bioactive Ceramic Material," *Bioceramics Development and Applications*, **6** (2016) 1-6.

31. L.L. Hench, R.J. Splinter, W.C. Allen, T.K. Greenlee. "Bonding Mechanisms at the Interface of Ceramic Prosthetic Materials" *Journal of Biomedical Materials Research*, **5 (6)** (1971)117-141.

32. O. Bretcanu, X. Chatzistavrou, K. Paraskevopoulos, R. Conradt, I. Thompson, A. R. Boccaccin, "Sintering and Crystallisation of 45S5 Bioglass Powder," *Journal of the European Ceramic Society*, **29(16)** (2009) 3299-3306.

33. I. B. Leonor, R. A. Sousa, A. M. Cunha, R. L. Reis, Z. P. Zhong, D. "Greenspan. Novel Starch Thermoplastic/Bioglass Composites: Mechanical Properties, Degradation Behavior and In-vitro Bioactivity," *Journal of Materials Science: Materials in Medicine*, **13 (10)** (2002) 939-945.

34. L. L. Hench, "Bioceramics: From Concept to Clinic," *Journal of the American Ceramic Society*, **74 (7)** (1991) 1487-1510.

35. P. Ducheyne, Q. Qiu, “Bioactive Ceramics: The Effect of Surface Reactivity on Bone Formation and Bone Cell Function,” *Biomaterials* **20** (1999) 2287-2303.

36. H. Oonishi, L. L. Hench, J. Wilson, E.S. Tsuji, M. Matsuura, “Quantitative Comparison of Bone Growth Behavior In Granules of Bioglass, A-W Glass-Ceramic, and Hydroxyapatite,” *Journal of Biomedical Materials Research,* **51(1)** (2000) 37-46.

37. N. M, Kotani, S. Nakamura, T. Yamamuro, T. Ohtsuki, C. Kokubo, T. Y. Bando, “A Comparative Study of Ultrastructures of the Interfaces Between Four Kinds of Surface-Active Ceramic and Bone,” *Journal of Biomedical Materials Research,* **26** (1992) 1419-1432.

38. K Yuan, K.C. Chen, Y.J. Chan, C.C. Tsai, H.H. Chen, C.C. Shih, “Dental Implant Failure Associated With Bacterial Infection and Long-Term Bisphosphonate Usage: *implant Dental,* **21** (2012) 3–7.

39. J.B. Wachtman, W.R. Cannon, M.J. Matthewson, “Mechanical Properties of Ceramics,” *ISBN: 978-0-470-45150-2* **2nd Edition,** (2009).

40. D. Broek, “Elementary Engineering Fracture Mechanics, 4th ed.,” *Martinus Nijhoff, Dordrecht,* (1987).

41. E. P. Butler, and E. R Fuller. “Ceramic-Matrixin Kirk–Othmer Encyclopedia of Chemical Technology,” *Composite Materials,* **4th ed. 7** (1993) 77–108.

42 M. W. Barsoum, “Fundamentals of Ceramics,” *Taylor & Francis group,* (2003).

43. S. X. Gong, “On the Formation of near-tip Microcracking and Associated Toughening Effects,” *Engineering Fracture Mechanics – Journal,* **50** (1995) 29-39.

44. S.T. Buljan, H.A. mckinstry, V.S. Stubican, “Optical and X-Ray Single Crystal Studies of the Monoclinic↔Tetragonal Transition in ZrO_2,” *Journal of the American Ceramic Society,* **59** (1976) 351.

45. A. G. Schneider, “Influence of Electric Field and Mechanical Stresses on the Fracture of Ferroelectrics,” *Annual Review of Materials Research*, **37** (2007) 491–538

46. A. J. Moulson, J. M. Herbert, Electroceramics Second addition, *Wiley*, (2003).

47. D. Berlincourt, H. A. H. Krueger, “Domain Processes in Lead Titanate Zirconate and Barium Titanate Ceramics,” *Journal of Applied Physics,* **30** (1959) 1804.

48. H. H. A. Krueger, D. Berlincourt, Effects of High Static Stress on the Piezoelectric Properties of Transducer Materials, *Journal of the Acoustical Society of America*, **33** (1961) 1339.

49. H. H. A. Krueger, “Stress Sensitivity of Piezoelectric Ceramics: Part 1. Sensitivity to Compressive Stress Parallel to the Polar Axis,” *Journal of the Acoustical Society of America*, **42** (1967) 636.

50. H. H. A. Krueger, “Stress Sensitivity of Piezoelectric Ceramics: Part 2. “Heat Treatment,” *Journal of the Acoustical Society of America,* **43** (1968) 583.

51. S.C. Hwang, C.S. Lynch, R.M. McMeeking, “Ferroelectric/Ferroelastic Interactions and a Polarization Switching Model,” *Acta Metallurgica et Materialia*. **43** (1995) 2073–2084.

52. R. K. N. D. Rajapakse, X. Zeng, “Toughening of Conducting cracks due to Domain Switching,” *Acta Materialia,* **49** (2001) 877.

53. C. Chandler, H. G. Fulton, “Effect of Local Polarization Switching On Piezoelectric Fracture*,” Journal of the Mechanics and Physics of Solids,* **49** (2001) 927.

54. A. B. K. Njiwa, T. Fett, D. C Lupascu, J. Rödel, “Effect of Geometry and Electrical Boundary Conditions on R-Curves For Lead Zirconate Titanate Ceramics,” *Engineering Fracture Mechanics,* **73(3)** (2006) 309–317.

55. W. Yang, F. Fang, M. Tao, “Critical Role of Domain Switching on Fracture Toughness of Poled Ferroelectrics,” *International Journal of Solids and Structures,* ***38*** (2001) 2203-2211.

56. M.G. Shaikh, S. Phanish, S.M. Sivakumar, “Domain Switching Criteria For Ferroelectrics,” *Computational Materials Science,* **37**(2006) 178–186.

57. Y. C.W. Yang, “Toughening under non-uniform Ferro-elastic domain switching,” *International Journal of Solids and Structures,* **43** (2006) 4452-4464.

58. F. Meschke, A. Kolleck and G. A. Schneider, “R-Curve Behaviour of BaTiO3 due to Stress-Induced Ferroelastic Domain Switching,” *Journal of the European Ceramic Society* **17** (1997) 1143-l 149.

59. W. Yang, T. Zhu, “Switch-toughening of Ferroelectrics Subjected to Electric fields,” *Journal of the Mechanics and Physics of Solids,* **46** (1998) 291–311.

60. M.J. Busche, K.J. Hsia, “Fracture and Domain Switching By Indentation In Barium Titanate Single Crystals” *Scripta Materialia,* **44** (2001) 207–212.

61. Z.A. Munir, U. A. Tamburini, M. Ohyanagi, “The Effect of Electric Field And Pressure on The Synthesis and Consolidation of Materials: A Review of The Spark Plasma Sintering Method.” *Journal of material science,* **41, (**2006) 763–777.

62. I.W. Chen, X.H. Wang, “Sintering Dense Nanocrystalline Ceramics Without Final-Stage Grain Growth,” *Nature,* **404** (2000) 168–171.

63. F.W. Dynys, J.W. Halloran, “Influence of Aggregates on Sintering,” *Journal of the American Ceramic Society,* **67** (1984) 596–601.

64. W.H. Tuan, E. Gilbart, R.J. Brook, “Sintering of Heterogeneous Ceramic Compacts” *Journal of material science,* 24 (1989) 1062–1068.

65. S. Rattanachan, Y. Miyashita, Y. Mutoh, “Effect of Polarization on Fracture Toughness of BaTiO3/Al2O3 Composites,” *Journal of the European Ceramic Society,* **24** (2004) 775–783.

66. K. M. Reddy, N. Kumar, B.tBasu, “Innovative multi-stage spark plasma sintering to obtain strong and tough ultrafine-grained ceramics,” *Scripta Materialia,* **62** (2010) 435–438.

67. A.K. Dubey, E.A. Anumol, K. Balani, B. Basu. “Multifunctional Properties of Multistage Spark Plasma Sintered HA–BaTiO3 Based Piezobiocomposites For Bone Replacement Applications,” *Journal of the American Ceramic Society*, **96(12)** (2013) 3753–3759.

68. S. Rattanachan, Y. Miyashita, Y. Mutoh, Microstructure And Fracture Toughness Of A Spark Plasma Sintered Al2O3-Based Composite with BaTiO3 Particulates, *Journal of the European Ceramic Society,* **23** (2003) 1269–1276.

69. G.D. Zhan, J. K., Julin, W. J. Garay, A. K. Mukherjee, “Spark-Plasma-Sintered $BaTiO_3/Al_2O_3$ Nanocomposites,” *Materials Science and Engineering A,* **356** (2003) 443-446.

70. T. Zhu, W. Yang, “Toughness Variation of Ferroelectrics by Polarization Switch Under Non-Uniform Electric Field, *Acta Materialia*, **45** (11) (1997) 4695-4702.

71. K. Zhang, F. W. Zeng, H. T. Lin, “Strength Properties of Aged Poled Lead Zirconatetitanate Subjected To Electromechanical Loadings,” *Smart Material Structure,* **21** (2012).

72. X. F. Li, K. Y. Lee, “Electric and Elastic Behaviors of a Piezoelectric Ceramic with a Charged Surface Electrode,” *Smart Material Structure,* **13** (2004) 424–432.

73. Y. W. Li, X. L. Zhou, and F. X. Li, “Ferroelastic Domain Switching In Lead Titanate zirconate ceramics: Temperature Dependence and Fracture Toughness Variations,” *Materials Science and Engineering,* **18** (2011).

74. W. Yang , T. Zhu, “Switch-Toughening of Ferroelectrics Subjected to Electric fields,” *Journal of the Mechanics and Physics of Solids,* **46 (2)** (1998) 291-311.

75 . Y.G. Liu, D.C. Jia, Y. Zhou, “Microstructure and Mechanical Properties of A Lithium Tantalate-Dispersed-Alumina Ceramic Composite,” *Ceramics International,* **28** (2002) 111–114.

76. X. Scott, M X. Lib, X. Hanb, “Toughening of Ferroelectric Ceramics under Polarization Switching, *Materials Science and Engineering A,* **292** (2000) 66–73.

77. S. Rattanachan, Y. Miyashita, Y. Mutoh, “Fracture Toughness of $BaTiO_3$-MgO Composites Sintered By Spark Plasma Sintering,” *Fracture Mechanics of Ceramics,* **14** 287-295.

78. Y.K. Baek, C.H. Kim, “The Effect of Whisker Length on The Mechanical Properties of Alumina-Sic Whisker Composites,” *Journal of Materials Science,* **24** (1989) 1589-1593.

79. Z. Zhang, L. Zhou, Y. H. L. Jiang, “Preparation and Characterization of Al_2O_3–$LaNbO_4$ Composites,” *Scripta Materialia*, **47** (2002) 637–641.

80. S.B. Park, C.T. Sun, “Effect of Electric Field on Fracture of Piezoelectric Ceramics,” *International Journal of Fracture,* **70** (1995) 203-216.

81. A. Kishimoto, S. Seo, “Strength Control of a Ceramic Composite by Electric Field,” *Smart Materials,* **4234** (2001) 321–327.

82. W. Lu, D.N. Fang, K.C. Hwang, “Micromechanics of Ferroelectric Domain Swihing Behavior Part I: Coupled Electromechanical Field of Domain Inclusions,” *Theoretical and Applied Fracture Mechanics,* **37** (2001) 29–38.

83. J. A. Mun˜oz-Tabares, E. Jime´nez-Pique, J. Reyes-Gasga, M. Anglada, "Microstructural Changes In Ground 3Y-TZP And Their Effect On Mechanical Properties," *Acta. Materialia,* 59 (2011) 6670–6683.

84. B. Yang, X.M. Chen, X.Q. Liu, "Effect of $BaTiO_3$ Addition on Structures and Mechanical Properties of 3Y-TZP Ceramics," *Journal of the European Ceramic Society,* **20** (2000) 1153-1158.

85. J. Li , B. Cui , H. Wang , Y. Lin, X. Deng , M. Li, C. Nan, "The Effects of Spark-Plasma Sintering (SPS) on the Microstructure and Mechanical Properties of BaTiO3/3Y-TZP Composites," *Materials,* **9 (5)** (2016) 320.

86. X. M. Chen, X.Q. Liu, F. Liu, X.B. Zhang, 3Y-TZP "Ceramics Toughened by Sr2Nb2O7 Secondary Phase," *Journal of the European Ceramic Society,* **21** (2001) 477–481.

87. T. Tanimoto, K. Okazaki, K. Yamamoto, "Tensile Stress-Strain Behavior of Piezoelectric Ceramics." *Japanese Journal of Applied Physics,* **32** (1993) 4233-4236.

88. D. J. Kim, "Effect of Ta_2O_5, Nb_2O_5, and HfO_2 Alloying on the Transformability of Y_2O_5-Stabilized Tetragonal ZrO_2," *Journal of the American Ceramic Society,* **73(1)** (1990) 115-120.

89. R. M. Mcmeeking, A.G. Evans, "Mechanics of Transformation Toughening in Brittle Materials," *Journal of the American Ceramic Society,* **65** (1982) 242–246.

90. X.Q. Liu, X.M. Chen, "Microstructures And Mechanical Properties of 8Y-FSZ Ceramics with BaTiO3 Additive," *Ceramics International,* **30** (2004) 2269–2275.

91. Y.G. Liu, D.C. Jia, Y. Zhou, M.H. Fang, Z.H. Huang, "In Situ TEM Observation Of Crack Propagation in $LiTaO_3$ Particle Toughened Al_2O_3 Ceramics," *Ceramics International,* **37** (2011) 647–650

92. T. L. Baker, K. T Faber, D. W. Readey, “Ferroelastic Toughening in Bismuth vanadate.” *Journal of the American Ceramic Society*, **74(7) (**1991), 1619-1623.

93. A.B. Schaufele, K.H. Hardtl, “Ferroelastic Properties of Lead Zirconate Titanate Ceramics” *Journal of the American Ceramic Society*, **79 (10)** (1996) 2637– 2640.

94. G.A. Schneider, V. Heyer, “Influence of the Electric Field On Vickers Indentation Crack Growth in BaTiO3” *Journal of the European Ceramic Society,* **19 (6–7)** (1999) 1299–1306.

95. R. F. Cook, B. R. Lawn, and, C. J. Fairbanks, “Microstructure-Strength Properties In Ceramics 1: Effect of Crack Size on Toughness,” *Journal of the American Ceramic Society*, **68** (11) (1985) 604-615.

96. Z. Zhang, and R. Rash, “Influence of Grain Size on Ferroelastic Toughening And Piezoelectric Behavior Of Lead Zirconate Titanate.” *Journal of the American Ceramic Society*, **78 (12)** (1995) 3363-3388.

97. R. F. Cook, S. W. Freiman, B. R. Lawn, R. C Pohanka, “Fracture of ferroelectric ceramics,” *Ferroelectrics,* **50** (1983) 267-272.

97. D. Berlincourt, H. H. A. Krueger, “Domain Processes in Lead Titanate Zirconate and Barium Titanate Ceramics” *Journal of Applied Physics,* **30** (1959) 1804.

98. Z. Liu, D. Fang , H. Xie, J. J. Lee, Study of effect of 90° domain switching on ferroelectric ceramics fracture using the moire´ interferometry, *ActaMaterialia* 55 (2007) 3911–3922.

99. C. Xiao, H. Zhang, L. Zhu, Z. Li, “Effect of $BaTiO_3$ addition on mechanical properties of $BaTiO_3/Al_2O_3$Composite,” *Applied Mechanics and Materials,* **422** (2013) 57-61.

100. G. A. Schneider, “Influence of Electric Field and Mechanical Stresses on the Fracture of Ferroelectrics,” *Annual Review of Materials Research,* **37** (2007) 491–538

101. A. L. Boskey., “Bone composition: relationship to bone fragility and anti-osteoporotic drug effects”, *International Bone & Mineral Society*, **447** (2013).

102. A. E. Ghannam, “Bone reconstruction: from bioceramics to tissue engineering,” *Expert Review of Medical Devices,* **2** (2005) 87-101.

103. G. B. Reinish, A. S. Nowick, “Effect of Moisture on the Electrical Properties of Bone,” *Journal of Electrochemical Society*, (10), **123** (1976)1451-145.

104. O. Kaygilia, S.V. Dorozhkinb, T. Atesa, A.A. Al-Ghamdic, F. Yakuphanoglua, “Dielectric Properties of Fe Doped Hydroxyapatite Prepared by Sol–Gel Method,” *Ceramics International*, **40** (2014) 9395-9402.

105. H.F.Cook “The dielectric behaviour of some types of human tissues at microwave frequencies”. *British Journal of Applied Physics* **2.10** (1951) 292-300.

106. T.S. England, “Dielectric Properties of the Human Body for Wave-lengths in the 1–10 cm. Range,” *Nature*, **166**(1950)480-481.

107. S. Singh, S. Saha “Electrical Properties of Bone: A Review”. *Clinical Orthopaedics and Related Research,* **186** (1984) 249-271

108. M.H. Shames, L.S. Lavine, “Physical Bases for Bioelectric Effects in Mineralized Tissues,” *Clinical Orthopaedics and Related Research,* **35**(1964)177-188.

109. J. Behari, H. Kumar ,R. Aruna, “Effect of Ultraviolet Light on the Dielectric Behavior of Bone at Microwave Frequencies,” *Annals of Biomedical Engineering*, (3), **10**(1982)139-144.

110. X. Wei, M.Z. Yates, “Yttrium-doped Hydroxyapatite Membranes with High Proton Conductivity,” *Chemistry of Materials*, **24** (2012) 1738-1743.

111. S.L. Shi, W. Pan, R.B. Han, C. L. Wan, “Electrical and Dielectric Behaviors of Ti3SiC2 /Hydroxyapatite Composites,” *Applied Physics Letters*, **88** (2006) 052903.

112. C. R. Bowen, A.J. Gittings, I.G. Turner, “Dielectric and Piezoelectric Properties of Hydroxyapatite-BaTiO3 Composites,” *Applied Physics Letters*, **89** (2006) 132906

113. A. K. Dubey, B. Basu, K. Balani, R. Guo, A. S. Bhalla, “Multifunctionality of Perovskites BaTiO3 andCaTiO3 in a Composite with Hydroxyapatite as Orthopedic Implant Materials,” *Integrated Ferroelectrics,* **131** (2011) 119-126.

114. N. Pisitpipathsin, P. Kantha, S. Eitsayeam, G. Rujijanakul, R. Guo, A.S. Bhalla, K. Pengpat, “Effect of BCZT on Electrical Properties and Bioactivity of 45S5 Bioglass,” *Integrated Ferroelectrics*, **142** (2013) 144-153.

115. S. Tigunta, N. Pisitpipathsin, P. Kantha, S. Eitssayeam, G. Rujijanagul, T. Tunkasiri, K. Pengpat, “Electrical Properties of Calcium Phosphate/BZT Bioglass-Ceramics Prepared by Incorporation Method,” *Ferroelectrics*, **459** (2014) 188-194.

116. H Porwal, S Grasso, L Cordero-Arias, C Li, A.R. Boccaccini, M.J. Reece, “Processing and Bioactivity of 45S5 Bioglass_-Graphene Nanoplatelets Composites,” *Journal of Materials Science: Materials in Medicine*, **25(6)** (2014) 1403-1413.

117. FME Eldin, NA El Alaily, “Electrical Conductivity of Some Alkali Silicate Glasses,” *Materials chemistry and physics,* (2), **52** (1998)175-179.

118. J.O. Bockris, J.A. Kitchner, S. Ingnotoutice, T.M. Tomlinson, “Electric Conductance in Liquid Silicates,” *Transactions of Faraday Society*, **48** (1952) 75-91.

119 A. Obata, S. Nakamura, K. Yamashita, “Interpretation of Electrical Polarization and Depolarization Mechanisms of Bioactive Glasses in Relation to Ionic Migration,” *Biomaterials,* **25** (2004) 5163-5169.

120 A. Jalalian, A. M. Grishin, "Biocompatible ferroelectric (Na, K) NbO3 nanofibers." *Applied Physics Letters* (1), **100** (2012) 012904.

121 K. Kakimoto , Y. Hayakawa, I. Kagomiya, "Low-Temperature Sintering of Dense (Na,K)NbO3Piezoelectric Ceramics Using the Citrate Precursor Technique," *Journal of the American Ceramic Society*, **93** (2010) 2423-2426

122 S. Swain, R.N. Padhy, T.R. Rautray, "Polarized Piezoelectric Bioceramic Composites Exhibit Antibacterial Activity," *Materials Chemistry and Physics*, **239** (2020) 122002.

123. S. Kumar, R. Vaish, S. Powar, "Surface-Selective Bactericidal Effect of Poled Ferroelectric Materials," *Journal of Applied Physics*, (1-6), **124** (2018) 014901.

124. G. Harkes, J. Feijen, J. Dankert, "Adhesion of E Werichia COD on to a Series of Poly (methacrylates) Differing in Charge and Hydrophobicity," *Biomaterials*, **12** (1991) 853-860.

125. E. Kłodzinska, M. Szumski, E. Dziubakiewicz, K. Hrynkiewicz, E. Skwarek, W. Janusz, B. Buszewsk, "Effect of Zeta Potential Value on Bacterial Behavior During Electrophoretic Separation," *Electrophoresis*, **31** (2010) 1590-1596.

126. R. Sonohara, N. Muramatsu, H. Ohshima, T. Kondo, "Difference in Surface Properties Between Escherichia coli and Staphylococcus aureus as Revealed by Electrophoretic Mobility Measurements," *Biophysical Chemistry*, (3), **55** (1995) 273-277.

127. M.P. Murphy, A. Holmgren, N.G. Larsson, B. Halliwell, C.J. Chang, B. Kalyanaraman, S.G. Rhee, P.J. Thornalley, L. Partridge, D. Gems, T. Nyström, "Unraveling the Biological Roles of Reactive Oxygen Species," *Cell metabolism*, **(4), 13** (2011) 361-366.

128. X.Q. Chen, X.Z. Tian, I. Shin, J. Yoon, "Fluorescent and Luminescent Probes for Detection of Reactive Oxygen and Nitrogen Species," *Chemical Society Reviews*, **(9), 40** (2011) 4783-4804.

129. G. Tan, S. Wang, Y. Zhu, L. Zhou, Yup, X. Wang, T. He, J. Chen, C. Mao, C. Ning, "Surface-Selective Preferential Production of Reactive Oxygen Species on Piezoelectric

Ceramics for Bacterial Killing," *ACS Applied Materials & Interfaces*, (37), **8** (2016) 24306-24309.

130. T. Yao, J. Chen, Z. Wang, J. Zhai, Y. Li, J. Xing, S. Hu, G. Tan, S. Qi, Y. Chang, P. Yu, C. Ning, "The Antibacterial Effect of Potassium-Sodium Niobate Ceramics Based on Controlling Piezoelectric Properties," *Colloids and Surfaces B: Biointerfaces*, **175**(2019) 463-468.

131. YH Leung, AMC Ng, X Xu, Z Shen, LA Gethings, M.T. Wong, C.M.N. Chan, M.Y. Guo, Y.H. Ng, A.B. Djurisic, P.K.H. Lee, W.K. Chan, L.H. Yu, D.L. Phillips, A.P.Y. Ma, F.C.C. Leung, "Mechanisms of Antibacterial Activity of MgO: Non-ROS Mediated Toxicity of MgO Nanoparticles Towards Escherichia coli," *Small*, **10** (2014)1171-1183.

132. A. Sirelkhatim, S. Mahmud, A. Seeni, N.H.M. Kaus, L.C. Ann, S.K.M. Bakhori, H. Hasan, D. Mohamad, "Review on Zinc Oxide Nanoparticles: Antibacterial Activity and Toxicity Mechanism, *Nano-Micro Letters*, **7** (2015)219-242.

133. A. Kumar, P.K. Vemula, P.M. Ajayan, G. John, "Silver-Nanoparticle-Embedded Antimicrobial Paints Based on Vegetable Oil," *Nature Materials*, **7 (3)** (2008)236-241.

134. T. Tian, C. Wu, J. Chang, "Preparation and In vitro Osteogenic, Angiogenic and Antibacterial Properties of Cuprorivaite (CaCuSi4O10, Cup) Bioceramics," *RSC Advances*, **6** (2016)45840-45849.

135. M.A.F. Afzal, S. Kalmodia, P. Kesarwani, B. Basu, K. Balani, "Bactericidal Effect of Silver-Reinforced Carbon Nanotube and Hydroxyapatite Composites," *Journal of Biomaterials Applications*, **27 (8)** (2013)967-978.

136. A. Pandey, S. Midha, R.K. Sharma, R. Maurya, V.K. Nigam, S. Ghosh, K. Balani, "Antioxidant and Antibacterial Hydroxyapatite-based Biocomposite for Orthopedic Applications," *Materials Science and Engineering: C*, **88** (2018)13-24

137. L. Grenho, C.L. Salgado, M.H. Fernandes, F.J. Monteiro, M.P. Ferraz, "Antibacterial Activity and Biocompatibility of Three-Dimensional Nanostructured Porous Granules of Hydroxyapatite and Zinc Oxide Nanoparticles an In Vitro and In Vivo Study," *Nanotechnology*, **26 (31)** (2015) 315101

138. S. K.Boda, I.Bajpai, B. Basu, "Inhibitory Effect of the Direct Electric Field and HA-ZnO Composites on S. Aureus Biofilm Formation," *Journal of Biomedical Materials Research Part B*, **104 (6)** (2016)1064-1075.

139. M. Ueshima, S. Nakamura, M. Ohgaki, K. Yamashita, "Electrovectorial Effect of Polarized Hydroxyapatite on Quasi-epitaxial Growth at Nano-interfaces," *Solid State Ionics*, **151** (2002)29-34.

140. M. Bellantone, N.J. Coleman , L.L. Hench , "Bacteriostatic Action of a Novel Four-Component Bioactive Glass," *Journal of Biomedical Materials Research,* , **51(3)** (2000) 484-90.

141. M. Kawashita, S. Tsuneyama, F. Miyaji, T.Kokubo, H. Kozuka, K.Yamamoto, "Antibacterial Silver-Containing Silica Glass Prepared by Sol–Gel Method," *Biomaterials*, **21 (4)** (2000)393-398.

142. K. Jurczyk, M.M. Kubicka, M. Ratajczak, M.U. Jurczyk, K. Niespodziana, D.M. Nowak, M. Gajecka, M. Jurczyk, "Antibacterial Activity of Nanostructured Ti−45S5 Bioglass−Ag Composite against Streptococcus mutans and Staphylococcus aureus," *Transactions of Nonferrous Metals Society of China,* , **26(1)** (2016) 118-125.

143. L. Percival, P.G. Bowler, D. Russell, "Bacterial Resistance to Silver in Wound Care," *Journal of Hospital Infection,* **60 (1)** (2005)1-7.

144. F. Jianqing, Y. Huipin, Z. Xingdong, "Promotion of Osteogenesis by a Piezoelectric Biological Ceramic," *Biomaterials*, **18** (1997)1531-1534.

145.Y. Zhang, L. Chen, J. Zeng, K. Zhou, D. Zhang, "Aligned Porous Barium Titanate/Hydroxyapatite Composites with High Piezoelectric Coefficients for Bone Tissue Engineering," *Materials Science and Engineering C,* **39** (2014)143-149.

146. A.K. Dubey, B. Basu, "Pulsed Electrical Stimulation and Surface Charge Induced Cell Growth on Multistage Spark Plasma Sintered Hydroxyapatite-Barium Titanate Piezobiocomposite," *Journal of the American Ceramic Society,* **97(2)** (2014)481-489.

147. M. Ohgaki, T. Kizuki, M. Katsura, and K. Yamashita, "Manipulation of Selective Cell Adhesion and Growth by Surface Charges of Electrically Polarized Hydroxyapatite," *Journal of Biomedical Materials Research,* **57**(2001)366-73.

148. F R Baxter, I G Turner, C R Bowen, J P Gittings, J B. Chaudhuri , "An in vitro study of electrically active hydroxyapatite-barium titanate ceramics using Saos-2 cells" *Journal of Materials Science: Materials in Medicine***, 20** (2009):1697–1708.

149. T. Kobayashi, S. Nakamura, K. Yamashita, "Enhanced Osteobonding by Negative Surface Charges of Electrically Polarized Hydroxyapatite," *Journal of Biomedical Materials Research,* **57 (4)** (2001)477-484

150. S. Itoh, S. Nakamura, T. Kobayashi, K. Shinomiya, K. Yamashita, S. Itoh, "Effect of Electrical Polarization of Hydroxyapatite Ceramics on New Bone Formation," *Calcified Tissue International,* **78** (2006)133-142.

151. C.S. Liu, H.F. Shao, F.Y. Chen, H.Y. Zheng, "Rheological Properties of Concentrated Aqueous Injectable Calcium Phosphate Cement Slurry," *Biomaterials,* **27** (2006) 5003-13

152. M. Julien, I. Khairoun, R. Legeros, S. Delplace, P. Pilet, P. Weiss, G. Daculsi, J.M. Bouler, J. Guicheux, "Physico-Chemical–Mechanical and In Vitro Biological Properties of Calcium Phosphate Cements with Doped Amorphous Calcium Phosphates," *Biomaterials,* **28** (2007) 956-65.

153. E. Burguera, H.H.K. Xu, S. Takagi, L.C. Chow, “High Strength Hydroxyapatite Cement Based on Dicalcium Phosphate Dihydrate for Bone Repair,” *Journal of Biomedical Materials Research A,* **71** (2004)272-82.

154. R.P.D. Real, E. Ooms, J.G. Wolke, M. Vallet-Regi, J.A. Jansen, “In vivo Bone Response to Porous Calcium Phosphate Cement,” *Journal of Biomedical Materials Research,* **65** (2003) 30-36.

155. Z.Z. Wu, J. Zhang, T.Y. Chen, C.S. Liu, Z.W. Chen, “Experimental Study of a New Type of Cement on Tibia Plateau Fractures Treatment,” *Clin Med J China,* **12** (2005) 261-64.

156. Z.Z. Wu, J. Zhang, T.Y. Chen, L.J. Li, C.S. Liu, H. Guo, et al. “Experimental Study on Magnesium Phosphate Cement in Fracture Treatment,” *Chinese journal of reparative and reconstructive surgery*, **20 (9)** (2006) 912-915.

157. F. Wu, J. Wei, H. Guo, F. Chen, H. Hong, C. Liu, “Self-setting Bioactive Calcium–Magnesium Phosphate Cement With High Strength and Degradability for Bone Regeneration,” *Acta Biomaterialia,* **4** (2008) 1873-1884.

158. N. Koju, P. Sikder, B. Gaihre, S.B. Bhaduri, “Smart Injectable Self-Setting Monetite Based Bioceramics for Orthopedic Applications,” *Materials,* **11** (2018) 1258.

159 P. Duan, J. Shen, G. Zou, X. Xia, B. Jin, “Biomimetic Mineralization and Cytocompatibility of Nanorod Hydroxyapatite/Graphene Oxide Composites,” *Frontiers of Chemical Science and Engineering,* (4), 12(2018)798-805.

160 J. Zhu, H.M. Wong, K.W.K. Yeung, S.C. Tjong, “Spark Plasma Sintered Hydroxyapatite/Graphite Nanosheet and Hydroxyapatite/Multiwalled Carbon Nanotube Composites: Mechanical and in Vitro Cellular Properties,” *Advanced Engineering Materials*, (4), **13** (2011) 336-341.